



Since January 2020 Elsevier has created a COVID-19 resource centre with free information in English and Mandarin on the novel coronavirus COVID-19. The COVID-19 resource centre is hosted on Elsevier Connect, the company's public news and information website.

Elsevier hereby grants permission to make all its COVID-19-related research that is available on the COVID-19 resource centre - including this research content - immediately available in PubMed Central and other publicly funded repositories, such as the WHO COVID database with rights for unrestricted research re-use and analyses in any form or by any means with acknowledgement of the original source. These permissions are granted for free by Elsevier for as long as the COVID-19 resource centre remains active.



Research paper

Discovery of potent benzoxaborole inhibitors against SARS-CoV-2 main and dengue virus proteases

Nikos Kühn, Johannes Lang, Mila M. Leuthold, Christian D. Klein*

Medicinal Chemistry, Institute of Pharmacy and Molecular Biotechnology IPMB, Heidelberg University, Im Neuenheimer Feld 364, 69120, Heidelberg, Germany



ABSTRACT

The RNA viruses SARS-CoV-2 and dengue pose a major threat to human health worldwide and their proteases (M^{pro} ; NS2B/NS3) are considered as promising targets for drug development. We present the synthesis and biological evaluation of novel benzoxaborole inhibitors of these two proteases. The most active compound achieves single-digit micromolar activity against SARS-CoV-2 M^{pro} in a biochemical assay. The most active substance against dengue NS2B/NS3 protease has submicromolar activity in cells (EC_{50} 0.54 μ M) and inhibits DENV-2 replication in cell culture. Most benzoxaboroles had no relevant cytotoxicity or significant off-target inhibition. Furthermore, the class demonstrated passive membrane penetration and stability against the evaluated proteases. This compound class may contribute to the development of antiviral agents with activity against DENV or SARS-CoV-2.

1. Introduction

The ongoing global COVID-19 pandemic is caused by the severe acute respiratory syndrome coronavirus 2 (SARS-CoV-2), a positive-strand RNA virus [1]. As of May 2022, more than 520 million infections and about 6.3 million deaths related to SARS-CoV-2 have been confirmed [2]. Recently, a highly efficient inhibitor of SARS-CoV-2 M^{pro} (Nirmatrelvir, Paxlovid®) was approved for clinical use [3] and other promising candidates like S-217622 are in ongoing clinical studies [4].

Similar to SARS-CoV-2, dengue virus (DENV; family: *Flaviviridae*) poses a global threat to human health, with an estimated world-wide incidence of 390 million infections per year [5]. Dengue fever is considered to be a neglected tropical disease. DENV infections often cause flu-like symptoms but can develop into aggravated disease with lethal outcomes [6,7]. To date, no specific therapeutic agent has been approved for this virus.

There is a high unmet medical need for drugs against both RNA viruses. Viral proteases are attractive drug targets against numerous viruses, including DENV and SARS-CoV-2 [8,9]. The function of both viral proteases (DENV: serine protease NS3 together with the cofactor NS2B; SARS-CoV-2: cysteine protease (M^{pro})) is essential to cleave the viral polyproteins and generate offspring virions [8]. For activity and cleavage of proteins of SARS-CoV-2 a M^{pro} homodimer formation is needed [9].

In recent years, boron-containing compounds have received increased attention in medicinal chemistry, also in the area of protease inhibitors [10–12], particularly for serine, aspartyl and metalloproteases, the proteasome [11] and cysteine proteases [13].

A very important boronic acid motif in medicinal chemistry are benzoxaboroles [14]. Several derivatives of this heterocycle have been approved or evaluated in clinical trials (see Fig. 1). The leucyl t-RNA synthetase inhibitor tavaborole was approved for the topical treatment of nail fungus in 2014 [15]. Crisaborole is an anti-inflammatory PDE4 inhibitor that was approved for the treatment of atopic dermatitis in 2016 [16]. Acoziborole was studied in clinical trials for treatment of african sleeping sickness (trypanosomiasis) [17].

Boronic acid and benzoxaborole derivatives have already been investigated as viral protease inhibitors. Boronic acid peptides were described as potent DENV, WNV and ZIKV inhibitors [18–20]. Boronic acid, cyclic boronate and benzoxaborole inhibitors of HCV NS3 protease are known [21–25] and in 2004 Bacha et al. described the identification of phenylboronic acid inhibitors of SARS-CoV M^{pro} [13]. A sub-picomolar phenylboronic acid inhibitor of HIV-1 protease was disclosed in 2018 [26].

Inspired by these successes, we designed and synthesized several compounds with the benzoxaborole motif and tested them against the protease of DENV-2 and the main protease of SARS-CoV-2. We herein present the structure-activity relationships, off-target evaluation and

* Corresponding author.

E-mail address: c.klein@uni-heidelberg.de (C.D. Klein).



Fig. 1. Structures of benzoxaborole APIs.

enzymatic studies of the benzoxaborole inhibitor series. Initial screenings were performed in biochemical assays. In addition, for the DENV protease, we carried out a cellular assay (DENV2proHeLa) that had a crucial role in the discovery of potent monobasic and non-basic inhibitors of DENV and WNV proteases [27,28].

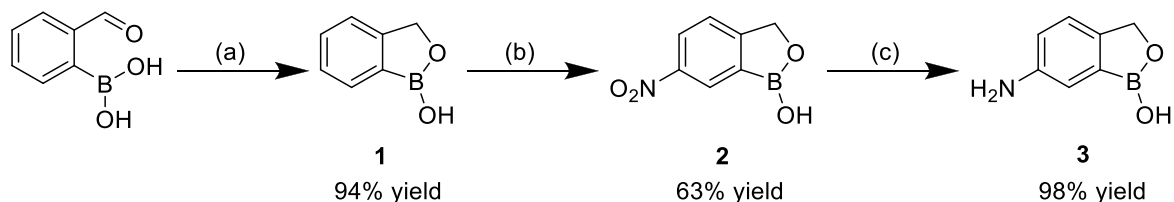
2. Results and discussion

Chemistry. The 6-aminobenzo[*c*][1,2]oxaborol-1(3*H*)-ol building block **3** was prepared on the basis of various literature syntheses (Scheme 1) [29–31]. For this purpose, 2-formylphenylboronic acid was reduced with sodium borohydride to the corresponding alcohol, which forms an ester with the boronic acid to yield the benzoxaborole heterocycle. By adding a mixture of concentrated nitric acid and sulfuric acid (1:2) at $-46\text{ }^{\circ}\text{C}$, the building block was selectively nitrated in the *meta* position. The resulting nitro compound was then reduced to the

corresponding aniline by the addition of elemental zinc and aqueous HCl.

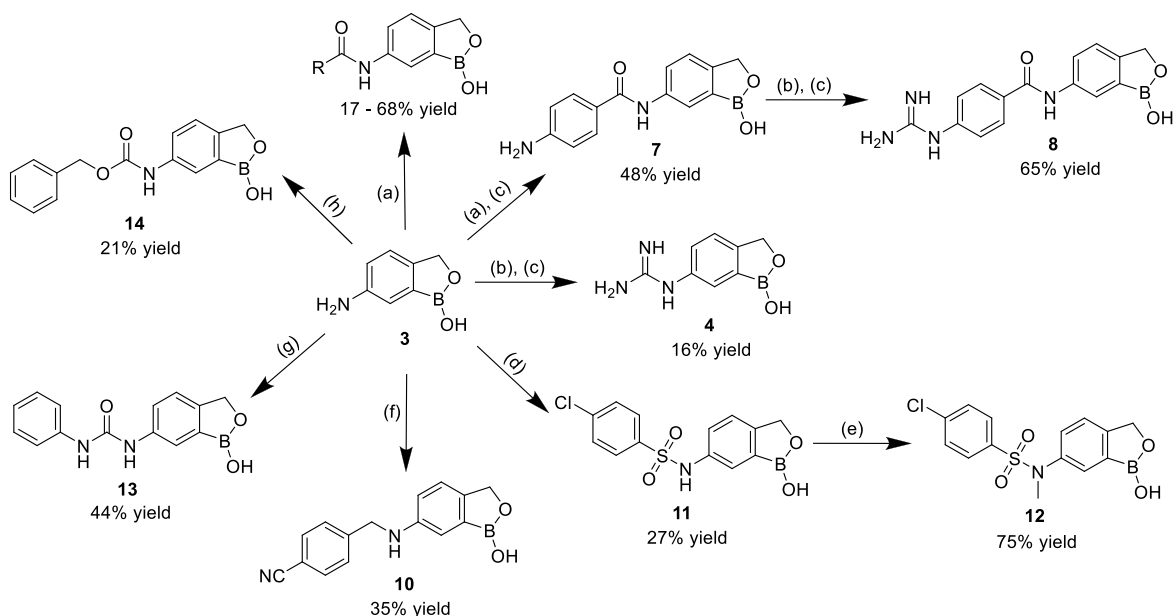
The amino group of the 6-aminobenzo[*c*][1,2]oxaborol-1(3*H*)-ol building block was used in several different reactions to yield amide, guanidine, sulfonamide, carbamate, urea and secondary amine derivatives (Scheme 2). Some of the synthesized compounds were further derivatized. Amide compounds were synthesized with the respective carboxylic acids, HATU as coupling reagent and TMP as base. All final compounds were purified by preparative RP-HPLC using ACN/H₂O (+0.1% TFA) followed by freeze-drying. Synthesis of intermediates like (benzyloxy)benzoic acid derivatives can be found in the Supporting Information.

Structure–Activity Relationships. The benzoxaboroles were primarily designed as inhibitors of the DENV serine protease NS3-NS2B. In the biochemical assay of DENV-2 and WNV protease, no relevant or only low activity could be observed for the compounds (Table S1). However,



Scheme 1. Synthesis of 6-Aminobenzo[*c*][1,2]oxaborol-1(3*H*)-ol

(a) NaBH₄, MeOH, 16 h; (b) HNO₃/H₂SO₄ (1:2, (V/V)), DCM, $-46\text{ }^{\circ}\text{C}$, 4 h; (c) Zn, aq. HCl, MeOH, 16 h.



Scheme 2. Synthesis of Benzoxaborole Compounds

(a) Respective carboxylic acid derivative, HATU, TMP, DCM/DMF, $0\text{ }^{\circ}\text{C} \rightarrow \text{r.t.}$, 16 h; (b) *N,N*-Di-Boc-1*H*-pyrazole-1-carboxamide, DMAP, DIPEA, MeOH, 2 days; (c) TFA/DCM (1:1); (d) 4-chlorobenzenesulfonyl chloride, DIPEA, DCM, $0\text{ }^{\circ}\text{C} \rightarrow \text{r.t.}$; (e) iodomethane, K₂CO₃, DMF, $0\text{ }^{\circ}\text{C} \rightarrow \text{r.t.}$; (f) 4-formylbenzonitrile, dry MeOH, 1 h, NaBH₃CN, overnight; (g) phenyl isocyanate, acetone, overnight; (h) benzyl chloroformate, DIPEA, DMAP, DCM, $0\text{ }^{\circ}\text{C} \rightarrow \text{r.t.}$

based on our previous experience with phenylglycine derivatives [27, 28], we nevertheless proceeded to test these compounds in the cellular DENV-2 protease reporter assay (DENV2proHeLa). This cellular reporter assay provides the full-length NS3 protein together with the NS2 cofactor in a natural environment without the need of an artificial linker, which is expected to influence protease conformations and dynamics [32] and therefore affects target-inhibitor recognition. Additionally, the cellular reporter gene assay incorporates additional factors such as permeability, metabolic stability and intracellular distribution and kinetics of the compounds [27]. Another possible explanation is the artificial composition of the biochemical assays of flaviviral protease activity. The assays are commonly performed at high pH values and high concentrations of additives (e.g. polyols, detergents) are used to achieve high enzymatic activity. Ehlert et al. demonstrated that the addition of nonionic detergents leads to significantly lower inhibition values [33]. Recently, Swarbrick et al. suggested that biochemical assays miss the inhibition of enzymatic autocleavage [34]. The activity of compounds that interfere with enzymatic autocleavage under native and cellular conditions may not be captured under biochemical conditions.

The benzoxaborole derivatives were also evaluated in a biochemical SARS-CoV-2 M^{PRO} assay as described before [35]. Cytotoxicity of the compounds was determined in DENV2proHeLa cells. Compounds **MB-53**, **NK-189**, boceprevir and MAC-5576 were included in the assays as reference inhibitors and had comparable activities to published values [27,35,36]. Structures of the reference compounds are provided in Fig. S1.

In Table 1, we provide the results of the biochemical SARS-CoV-2 M^{PRO} and the cellular DENV2proHeLa assays along with the cytotoxicity. Further biochemical testing data, including the off-targets trypsin and thrombin, is provided in the supplementary material (Tables S1 and S2). The synthetic intermediates benzo[*c*][1,2]oxaborol-1(3*H*)-ol (compound 1), the corresponding nitro and amino derivatives (compounds 2 and 3) and the leucyl-tRNA synthetase inhibitor tavaborole did not have inhibitory activity against both proteases (Table 1). The guanidine and the phenyl guanidine compounds 4 and 8 showed moderate potencies with IC₅₀ values of 10.0 and 13.9 μM against SARS-CoV-2 M^{PRO} in a biochemical assay. Such high level of activity was also expected against the DENV protease, which primarily favors basic residues in its active center [8]. However, the charge of the strongly basic guanidine group could impede penetration through the cell membrane, causing lower efficacy in a cellular setting. The other tested compounds without additional phenyl or benzyl residues showed no relevant activity against M^{PRO}. For the sulfonamide (11) and carbamate compounds (14) single-digit micromolar activity against DENV protease was found. Particularly interesting is the 3-methoxybenzoic acid derivative 9. It already reached an IC₅₀ value of 6.4 μM and the incorporation of a benzyl residue increased the activity against both viral proteases. Compound 18 had 2.5 times lower EC₅₀ value against DENV-2 compared to 9. Additionally, a potent IC₅₀ value of 6.2 μM against SARS-CoV-2 M^{PRO} was determined. The compound has therefore nearly 3-fold higher activity than boceprevir, which was previously considered as a promising structural starting point for SARS-CoV-2 drug substance development [37]. Compound 18 is thus more active against both proteases than the phenoxy compounds (15, 16) and the *ortho* and *para* benzyloxy derivatives (17, 19) tested. Incorporation of a 4-chloro substituent to the benzyl residue in compound 20 decreased the activity against both proteases significantly. Due to its similar structure to 3-phenoxybenzoic acid, the NSAID fenoprofen was tested as a structural element (compound 21). The inhibitory activity against DENV protease was comparable to 18, while it is almost completely lost against SARS-CoV-2 M^{PRO}. Exchanging the oxygen in the benzyloxy structure against nitrogen or an amide group led to a loss of activity against both targets. But these modifications also significantly reduced cytotoxicity of the compounds. Most interesting is the clear difference in activity of the benzoxaborole derivative 18 in comparison to the phenylboronic acid compounds 26 and 27. The phenylboronic acid compounds showed

nearly no activity against SARS-CoV-2 M^{PRO} and an approximately 5 to 6-fold lower inhibitory activity against the DENV protease, clearly indicating the importance of the benzoxaborole heterocycle.

It is surprising that compounds with activity against both proteases were found, since their structures, including the catalytic residue (Cys vs. Ser), and the substrate recognition preferences, of the two targets are very different [8,9]. This is particularly noteworthy since we do not see any indication of promiscuity or low selectivity: The compounds do not have significant cytotoxicity and do not inhibit the two off-target proteases trypsin and thrombin (Table S2). We therefore see potential to pursue a further development of these compounds as inhibitors of SARS-CoV-2 and DENV viruses. Murtuja et al. even suggested dual inhibitors against both proteases [38]. This strategy gains further attractiveness because co-infections with DENV and SARS-CoV-2 are an emerging public health concern [39]. However, due to the different structures and enzymatic mechanisms of these proteases it appears more promising to employ the benzoxaborole heterocycle as a common, “ancestral” building block for the development of distinct classes of inhibitors.

Most of the benzoxaborole compounds in Table 1 were only cytotoxic at very high compound concentrations, resulting in excellent selectivity indices. For some of the compounds, no influence on cell survival was found even at high concentrations of 100 or even 200 μM.

Since the *meta*-benzyloxybenzoic acid derivative 18 had the highest activity against both proteases, it was chosen as the starting point for a second round of structure-activity explorations (Table 2). All structural variations caused a significant reduction in inhibitory activity against SARS-CoV-2 M^{PRO}. The pyridine derivative 28 and the 3-((3-methylbenzyl)oxy) derivative 29 had IC₅₀ values of 38.5 and 59.8 μM, respectively. All other structural modifications of 18 led to IC₅₀ values of around or even over 60 μM. A more positive picture emerged from the DENV protease assays: Substitution with 3-methoxy (compound 30), 4-chloro (compound 32) or the exchange of the central phenyl ring to a pyridine ring (compound 28) led to comparable inhibition to compound 18. The 3-((4-cyanobenzyl)oxy) and the 3-(cyclohexylmethoxy) derivatives 31 and 34 showed slightly higher EC₅₀ values. An improvement in the inhibitory activity was reached by a 3-methyl and a 2,6-dichloro substitution. With compound 29 2-fold improvement could be achieved whereas compound 33 had a 4-fold lower EC₅₀ value. Compound 33 is therefore one of the most active DENV-2 protease inhibitors in cells and is in the same activity range as recently published inhibitors [27,28]. The substituents and structural variations of the 3-(benzyloxy) derivatives also had a major influence on the cytotoxicity of the compounds. Derivatives 28 (pyridine ring), 29 (3-methyl residue), 32 (4-chloro residue) and 34 (cyclohexyl ring) showed slightly lower cytotoxicity. The incorporation of a 3-methoxy residue in compound 30 or 4-cyano function in compound 31 led to CC₅₀ values above 200 μM. The most active compound against DENV NS2B/NS3, which has a 2,6-dichlorobenzyl residue (compound 33) had minimally higher cytotoxicity than compound 18. But even this compound still has an excellent selectivity index of 74.

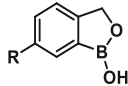
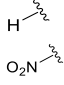
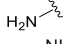
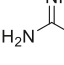
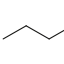
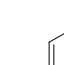
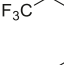
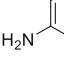
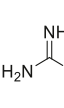
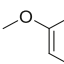
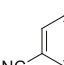
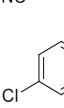
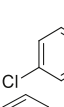
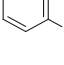
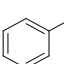
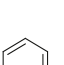
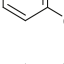
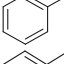
Enzymatic studies. Various enzyme kinetic measurements with SARS-CoV-2 M^{PRO} were carried out. Fig. 2A shows the dose-response curves of compounds 18, 4 and 8 with Hill slopes close to 1.

It was previously shown that inhibition of nonspecific promiscuous inhibitors is DTT-dependent [40]. We have therefore determined the inhibition of selected inhibitors with addition of 1 mM DTT to the assay buffer. The addition did not result in change of the inhibition values (Fig. S2).

Previously published phenylboronic acid inhibitors of SARS-CoV M^{PRO} were reported to bind noncompetitively to a serine-rich subsite close to the catalytic cysteine [13]. A noncompetitive binding behavior for the presented compounds is reasonable, especially because compounds 8 and 18 do not show competitive binding with SARS-CoV-2 M^{PRO}. This is demonstrated by the Cheng-Prusoff plots of the compounds in Fig. 2B. Since an increasing substrate concentration does not

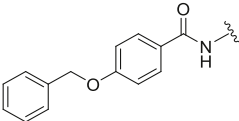
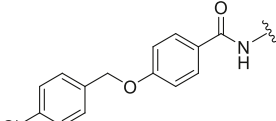
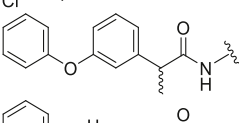
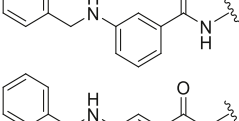
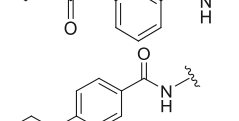
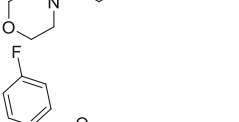
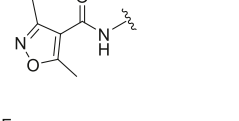
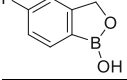
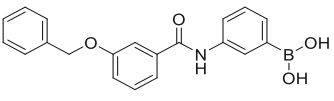
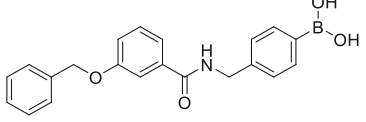
Table 1

Inhibitory activity of benzoxaboroles against SARS-CoV-2 main protease, in the cellular DENV-2 protease reporter gene assay (DENV2proHeLa), and cytotoxicity in DENV2proHeLa Cells.

Cpd.	R	SARS-CoV-2 M ^{Pro}		DENV2proHeLa ^b		CC ₅₀ (μM) ^c
		% (50 μM)	IC ₅₀ (μM) ^d	% (12.5 μM)	EC ₅₀ (μM)	
1		n.i.	n.d.	n.i.	n.d.	>100
2		n.i.	n.d.	14.5 ± 5.5	n.d.	>100
3		17.5 ± 4.1	n.d.	n.i.	n.d.	>100
4		88.0 ± 2.2	10.0 ± 0.5	n.i.	n.d.	>100
5		n.i.	n.d.	37.2 ± 12.4	19.2 ± 5.3	>200
6		21.0 ± 1.1	n.d.	n.i.	n.d.	>50
7		39.7 ± 2.8	n.d.	14.3 ± 5.4	n.d.	>200
8		87.4 ± 6.2	13.9 ± 0.7	23.0 ± 7.2	n.d.	>200
9		24.3 ± 3.2	n.d.	60.1 ± 3.9	6.4 ± 1.8	>100
10		n.i.	n.d.	41.8 ± 11.9	n.d.	>100
11		n.i.	n.d.	51.6 ± 5.9	9.2 ± 2.0	>50
12		n.i.	n.d.	24.2 ± 16.7	>50	>50
13		15.9 ± 4.9	n.d.	31.0 ± 4.5	22.5 ± 2.5	>200
14		n.i.	n.d.	67.5 ± 6.3	4.0 ± 0.7	>50
15		19.5 ± 8.5	n.d.	79.7 ± 5.3	3.5 ± 0.4	>50
16		34.6 ± 7.6	n.d.	77.4 ± 2.4	6.4 ± 1.5	>50
17		40.6 ± 5.2	n.d.	66.7 ± 2.3	6.1 ± 1.7	>50
18		99.6 ± 2.6	6.1 ± 0.5	81.2 ± 5.3	2.4 ± 0.1	55.2 ± 8.5

(continued on next page)

Table 1 (continued)

Cpd.	R	SARS-CoV-2 M ^{pro}		DENV2proHeLa ^b		CC ₅₀ (μM) ^c
		% (50 μM)	IC ₅₀ (μM) ^a	% (12.5 μM)	EC ₅₀ (μM)	
19		39.6 ± 6.7	n.d.	54.4 ± 5.0	8.8 ± 1.6	>50
20		20.4 ± 3.9	n.d.	31.3 ± 17.8	14.5 ± 3.1	>50
21		19.0 ± 1.5	n.d.	76.7 ± 15.0	3.1 ± 0.8	>50
22		46.9 ± 9.0	56.9 ± 6.2	73.6 ± 2.7	5.2 ± 0.4	144.1 ± 5.0
23		45.6 ± 7.4	52.3 ± 4.6	51.5 ± 4.5	13.1 ± 2.2	>200
24		12.7 ± 5.1	n.d.	41.1 ± 7.8	17.1 ± 4.7	>50
25		n.i.	n.d.	32.6 ± 8.4	21.6 ± 5.0	>100
Tavaborole		n.i.	n.d.	15.3 ± 10.3	n.d.	>50
26		n.i.	n.d.	65.1 ± 6.4	12.5 ± 1.9	>50
27		18.5 ± 8.2	n.d.	29.3 ± 5.9	14.0 ± 2.9	>50
reference compounds						
MB-53(Cpd. 27 in [36])		n.d.	n.d.	42.9 ± 7.0	19.6 ± 1.8	>50
NK-189(Cpd. 20 in [27])		n.d.	n.d.	79.3 ± 9.7	0.6 ± 0.1	>50
boceprevir [35]		70.8 ± 7.4	17.2 ± 1.5	n.d.	n.d.	n.d.
MAC-5576 [35]		95.0 ± 5.3	1.7 ± 0.0	n.d.	n.d.	n.d.

If inhibition ≤10% = no inhibition (n.i.). n.d. = not determined. All measurements were carried out in triplicate.

^a IC₅₀ values against SARS-CoV-2 at 25 μM substrate concentration.

^b Values against DENV serotype 2 protease in reporter gene assay in HeLa cells.

^c Measured in DENV2proHeLa cells.

influence the measured IC₅₀ of the compounds, competitive binding of inhibitors **8** and **18** can be excluded.

A Michaelis-Menten plot with different concentrations of compound **18** indicates a mixed inhibition mode (Fig. S3). With increasing inhibitor concentrations the V_{max} values decrease significantly, whereas the K_m values only change slightly. A K_i value of 6.2 μM for compound **18** was

calculated. Unfortunately, the exact binding location of the compounds remains unknown.

There is no significant increase or decrease in the inhibitory activity over time as shown with compounds **8** and **18** in Fig. 2C. Only a minimal difference was found between the incubation time points of 0 or 10 min. In any case, all biochemical activity measurements were carried out

Table 2

Inhibitory activity of benzoxaborole compounds with 3-(benzyloxy)benzoic acid motif against SARS-CoV-2 main protease, in the cellular DENV-2 protease reporter gene assay (DENV2proHeLa) and cytotoxicity in DENV2proHeLa cells.

Cpd.	R	SARS-CoV-2 M ^{pro}		DENV2proHeLa ^b		CC ₅₀ (μM) ^c
		% (50 μM)	IC ₅₀ (μM) ^a	% (12.5 μM)	EC ₅₀ (μM)	
18		99.6 ± 2.6	6.1 ± 0.5	81.2 ± 5.3	2.4 ± 0.1	55.2 ± 8.5
28		55.5 ± 7.0	38.5 ± 3.1	85.2 ± 4.1	2.5 ± 0.2	123.9 ± 16.1
29		45.7 ± 6.3	59.8 ± 4.7	90.0 ± 0.9	1.1 ± 0.1	72.6 ± 15.4
30		43.4 ± 9.1	n.d.	80.4 ± 2.0	2.9 ± 0.3	>200
31		31.7 ± 3.6	n.d.	82.2 ± 3.7	4.1 ± 0.2	>200
32		43.5 ± 9.7	n.d.	83.6 ± 1.7	2.4 ± 0.2	75.3 ± 9.4
33		32.6 ± 3.9	n.d.	85.6 ± 4.3	0.54 ± 0.05	39.7 ± 5.1
34		29.3 ± 7.5	n.d.	79.1 ± 1.5	3.4 ± 0.5	123.4 ± 2.4

If inhibition ≤10% = no inhibition (n.i.). n.d. = not determined. All measurements were carried out in triplicate.

^a IC₅₀ values against SARS-CoV-2 at 25 μM substrate concentration.

^b Values against DENV serotype 2 protease in reporter gene assay in HeLa cells.

^c Measured in DENV2proHeLa cells.

after an incubation time of 15 min.

A dilution experiment was carried out to show reversible binding of compound **18** (Fig. 2D). SARS-CoV-2 M^{pro} was preincubated with the inhibitor at a high concentration (100 μM) for 2 h. Afterwards, the inhibitor was diluted to one-half of its IC₅₀ value (3 μM) and the remaining activity of the enzyme was determined. Compound **18** shows slightly increased inhibition at time point 0 min in comparison to the one-half IC₅₀ control. After 15 min of incubation, no difference to the one-half IC₅₀ control was observed. It can therefore be concluded that the compound binds in a reversible manner to its target.

We were not able to detect mass adducts by ESI-TOF of benzoxaborole compounds with SARS-CoV-2 M^{pro}, but adducts were found with the reference compound boceprevir (data not shown). We conclude that either no covalent bond was formed between the benzoxaboroles and the target or that covalent-reversible adducts are formed, which are unstable under ESI ionization conditions.

Selectivity against Off-Targets. Boronic acid derivatives are known to inhibit several serine proteases effectively [11]. Therefore, all

compounds were screened against the potential off-targets thrombin and trypsin at a concentration of 50 μM (Table S2). Surprisingly, hardly any activity against the proteases could be determined, showing high selectivity of the compound class. In contrast, previously published boronic acid inhibitors of flaviviral proteases showed very potent activity against these off-targets [19]. Only phenyl guanidine compound **8** showed relevant activity against trypsin (IC₅₀ = 61.4 μM).

To exclude inhibition of the Renilla luciferase or cellular targets, we screened selected inhibitors in HeLa cells expressing the luciferase reporter construct but not the DENV-2 protease (Fig. S4). No influence on cell survival or luciferase signal could be detected, which excludes an inhibition or an influence on expression of the cellular reporter construct.

Antiviral Activity in DENV-2 Titer Reduction Assay. To confirm the activity of the compounds in the DENV2proHeLa assay, selected compounds and the reference inhibitor **NK-189** were screened in a DENV serotype 2 titer reduction assay. Huh-7 cells were infected with DENV-2 (MOI of 1) and treated with 12.5 μM of the compounds. The

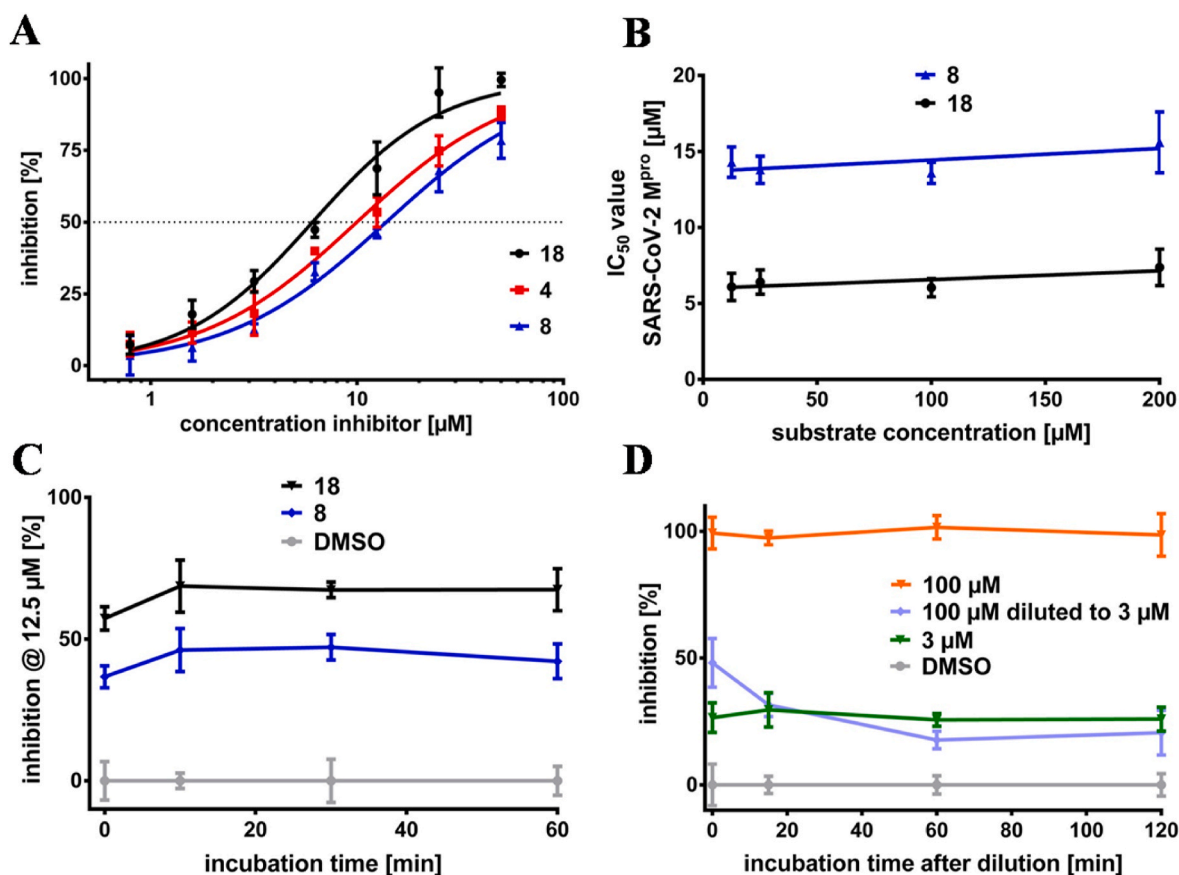


Fig. 2. Enzyme kinetic measurements with SARS-CoV-2 M^{pro}. (A) dose-response curves of compounds 18, 4 and 8. Hill slopes are 1.39 ± 0.16 , 1.15 ± 0.07 , 1.14 ± 0.07 , respectively. (B) Cheng-Prusoff plots of compounds 8 and 18. (C) Time dependent inhibition of compounds 18 and 8 at a concentration of 12.5 μM. (D) Dilution experiment for compound 18. Enzyme and inhibitor were incubated for 2 h. Inhibition values for 2C and 2D were determined after 5 min of measurement.

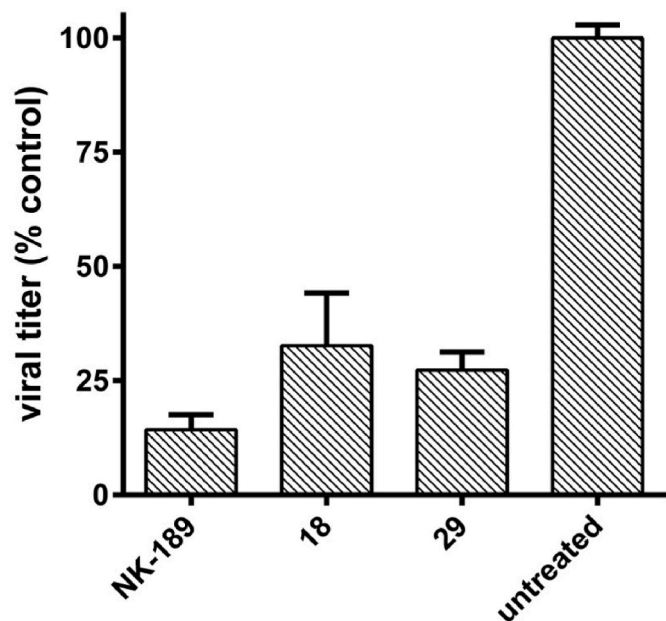


Fig. 3. Inhibitory activity of selected compounds and reference compound NK-189 at a concentration of 12.5 μM in a DENV-2 titer reduction assay. None of the compounds revealed cytotoxicity at the tested concentration.

tested compounds reduced the viral titer at the screening concentration (see Fig. 3). Compound 18 and 29 had antiviral activities of 67.4% and 72.6%, respectively. However, this activity was below that of the reference substance NK-189 (0.89 μM) [27]. The compounds were not cytotoxic for Huh-7 cells at the tested concentration.

2.1. Compound membrane permeability and stability against viral proteases

With the precoated trilayer parallel artificial membrane permeability assay (PAMPA) [41,42] the passive membrane permeability of selected benzoxaborole compounds and references were evaluated (Table S3). The permeability of the reference compounds was in accordance with published literature values [41]. Whereas compound 4 showed no permeability, compounds 11, 15, 17, 18, 20, 26, 31 and 33 revealed passive permeability. Compound 4 contains a highly basic guanidine structure, which can explain the low membrane penetration. The *para* cyano compound 31 showed less permeability than the unsubstituted derivative (compound 18), where the dichloro compound 33 showed significantly higher permeability. This can explain the different activity of the compounds in the cell-based DENV2proHeLa assay. Interestingly, benzoxaborole compound 18 and the phenylboronic acid analogue 26 showed comparable permeability values. However, compounds 15, 11, 17 and 20 had higher permeability than 18, which does not match to the significantly different potencies of the compounds in the cell-based assay. This deviation could be explained by differences in active membrane transport, compound metabolism and target affinity of the inhibitors.

Since it has already been shown for peptidic DENV inhibitors that they are partially cleaved by the DENV protease [43,44], selected

compounds from this work were examined for their stability against both viral proteases (Fig. S5). The compounds presented here are not peptidic, but do contain amide bonds that could be cleaved by the viral proteases. Compound **8**, **18** and **23** were incubated with SARS-CoV-2 M^{Pro} in the respective assay buffer. After 8 h of incubation, the quantity of compounds was analyzed by HPLC with an UV/Vis detector and no cleavage of the compounds was detected (Fig. S5A). The same was done for compounds **15**, **18**, **20** and **32** with the isolated DENV-2 protease in the DENV assay buffer. After 8 h of incubation, no decrease in the compound AUC could be detected by HPLC analysis (Fig. S5B). Therefore, stability of the tested compounds in the assay buffers and against the two viral proteases could be shown.

3. Conclusions

Benzoxaboroles represent a promising structure for the development of new protease inhibitors against RNA viruses. The newly described compound set offers an opportunity for the development of compounds with activity against the proteases of SARS-CoV-2 and DENV. Surprisingly, activity against two significantly different viral proteases was observed. While the single-digit micromolar activity against SARS-CoV-2 M^{Pro} was determined for compound **18**, the EC₅₀ values against DENV-2 protease was 2.4 μM in the cell-based DENVproHeLa assay. Enzyme kinetic measurements were performed to verify non-competitive and reversible binding of the benzoxaborole compounds against SARS-CoV-2 M^{Pro}. Structure-activity studies with various substitutes on the *meta*-benzyloxy residue led to a selective inhibition of the DENV protease and an increase in activity HeLa cells. DENV-2 titer reduction assays proved antiviral activity of the compound class. PAMPA measurements verified passive membrane penetration and stability measurements against the isolated viral proteases showed complete compound stability. In the tested concentration range, no relevant cytotoxicity against HeLa cells could be detected and only one compound of the compound set showed relevant inhibitory activity against the serine protease trypsin. Even at the high concentration of 50 μM no compound had inhibitory effects on the coagulation-catalyzing serine protease thrombin.

Future studies are necessary to further improve the activity against both targets. One approach is to develop an inhibitor with dual activity against both proteases as recently suggested [38] or to use the structures identified here to design inhibitors that exclusively inhibit one of the enzymes examined. In addition, further studies are planned to investigate the exact binding location and binding mode of the benzoxaborole compounds.

4. Experimental section

Reagents and Solvents. All chemicals for the synthesis of precursors were obtained from Sigma-Aldrich (Germany), Alfa Aesar (Germany), Thermo Fisher Scientific (Germany/United States), TCI Europe (Belgium), Carbolution Chemicals (Germany) and were of analytical grade. Boceprevir was obtained from Biosynth-Carbosynth (Bratislava, Slovak Republic). Ethyl acetate and deionized water were distilled prior to use. Other solvents were used as obtained from the commercial suppliers.

Equipment and Analytical Methods. The progress of the reactions was determined by thin layer chromatography (TLC) on Macherey-Nagel polygram SIL G/UV₂₅₄ polyester plates (UV detection). Flash chromatography was performed on a Biotage Isolera One purification system using silica gel (mesh 230–400, 60 Å) cartridges (KP-Sil) and UV monitoring at 254 and 280 nm. NMR spectra were recorded on Varian NMR instrument at 300 or 500 MHz, 300 K; Chemical shifts (δ) are given in parts per million (ppm). Residual peaks of nondeuterated solvents were used as internal standard: CD₃OD (δ ppm: 3.31), DMSO-*d*₆ (δ ppm: 2.50), CD₃CN (δ ppm: 1.94) and acetone-*d*₆ (δ ppm: 2.05). Coupling constants (*J*) are given in hertz (Hz). Multiplicity is reported as s (singlet), d (doublet), t (triplet), q (quartet), p (pentet), dd (doublet of

doublet), m (multiplet), and br (broad). The carbon attached to boron was not always observed due to the quadrupolar relaxation of ¹⁰B and ¹¹B nuclei. Mass spectra (HR-ESI) of all compounds were measured on a Bruker micrOTOF-Q II instrument. Analysis of the compounds and intermediates was carried out using solutions in water, methanol, acetonitrile, water/methanol or water/acetonitrile. Purity of inhibitors was determined by HPLC on a Jasco HPLC system with a Jasco UV-2070 Plus Intelligent UV/VIS Detector on an RP-18 column (ReproSil-Pur-ODS-3, Dr. Maisch GmbH, Germany, 5 μm, 50 mm × 2 mm). All final compounds were purified by preparative RP-HPLC on an ÄKTA pure 25 M, GE Healthcare (Germany), with an RP-18 pre and main column (Rephosphor, Dr. Maisch GmbH, Germany, C18-DE, 5 μm, 30 mm × 16 mm and 120 mm × 16 mm). The following conditions were used: eluent A, water (0.1% TFA); eluent B, methanol (0.1% TFA) or eluent A, water (0.1% TFA); eluent B, acetonitrile (0.1% TFA); flow rate, 8 mL/min; and gradient, 10% B (2.5 min), 100% B (23.5 min), 100% B (26 min), 10% B (26.1 min), and 10% B (30 min). Detection was performed at 214, 254, and 280 nm. After purification, the organic solvent was evaporated, and the compounds were freeze-dried in H₂O/ACN and stored at –20 °C. Lyophilization was performed with an “Alpha 1–2 LDplus” freeze-drier (Martin Christ, Germany). Reported yields of boronic acids are calculated based on the free acid form without consideration of anhydride formation. Purity for the final compounds is ≥ 95% unless indicated otherwise (see Table S4).

Benzo[*c*][1,2]oxaborol-1(3*H*)-ol (1). **1** was synthesized in analogy to previously published methods [29,45]. Sodium borohydride (396 mg, 10.5 mmol) was added to a solution of 2-formylphenylboronic acid (1499 mg, 10.0 mmol) in methanol (40 mL). The reaction mixture was stirred at room temperature overnight and on the next day 5 M aqueous HCl (50 mL) was added. The aqueous phase was extracted with Et₂O 3 times and the combined organic phases were dried over MgSO₄. The solvent was evaporated under reduced pressure to yield a colorless solid (1265 mg, 94% yield). ¹H NMR (300 MHz, DMSO-*d*₆) δ 9.14 (br s, 1H), 7.74 (d, *J* = 7.2 Hz, 1H), 7.54–7.30 (m, 3H), 4.98 (s, 2H). ¹³C NMR (APT, 75 MHz, DMSO-*d*₆) δ 153.9, 130.5, 130.5, 126.8, 121.3, 69.9. HRMS (ESI): *m/z* [M – H][–] calcd for C₇H₆BO₂: 133.0166, found: 133.0174.

6-Nitrobenzo[*c*][1,2]oxaborol-1(3*H*)-ol (2). **2** was synthesized in analogy to a previously published method [45]. To a cooled solution of 65% HNO₃ was added **1** (784 mg, 5.9 mmol) slowly at –46 °C. Twice the volume of H₂SO₄ (98%) was added slowly to the mixture under vigorous stirring. After completion of addition, the reaction mixture was stirred for 4 h. The mixture was quenched with the addition of crushed ice and warmed to room temperature slowly. The resulting yellow suspension was filtered, washed with cooled water and dried under reduced pressure to yield a yellow solid (659 mg, 63% yield). ¹H NMR (300 MHz, DMSO-*d*₆) δ 9.58 (s, 1H), 8.58 (s, 1H), 8.33 (d, *J* = 8.4 Hz, 1H), 7.70 (d, *J* = 8.3 Hz, 1H), 5.12 (s, 2H). ¹³C NMR (APT, 75 MHz, DMSO-*d*₆) δ 160.6, 147.2, 125.6, 125.5, 123.1, 70.1. HRMS (ESI): *m/z* [M – H][–] calcd for C₇H₅NO₄: 178.0318, found: 178.0310.

6-Aminobenzo[*c*][1,2]oxaborol-1(3*H*)-ol (3). **3** was synthesized in analogy to a previously published method [46]. To a suspension of **2** (298 mg, 1.7 mmol) in MeOH (15 mL) was added 2 M HCl (15 mL) and Zn dust (1090 mg, 16.6 mmol). The reaction mixture was stirred at room temperature for 6 h before it was neutralized by a solution of saturated aq. NaHCO₃. Ethyl acetate (50 mL) was added and the mixture was filtered through Celite and washed with ethyl acetate several times. The organic layer was washed with 5% aq. NaHCO₃, brine and dried over MgSO₄. The solvent was evaporated to dryness to yield **3** as a yellow solid (244 mg, 98% yield). To obtain the respective HCl salt, the compound was treated with a solution of HCl in dioxane (4 M). After removal of the solvent, a yellow solid was yielded. ¹H NMR (300 MHz, DMSO-*d*₆) δ 8.91 (s, 1H), 7.03 (d, *J* = 8.0 Hz, 1H), 6.90 (s, 1H), 6.70 (d, *J* = 8.0 Hz, 1H), 4.98 (s, 2H), 4.81 (s, 2H). ¹³C NMR (APT, 75 MHz, DMSO-*d*₆) δ 147.5, 141.4, 130.5, 121.4, 117.6, 114.6, 69.6. HRMS (ESI): *m/z* [M+H]⁺ calcd for C₇H₉NO₂: 150.0722, found: 150.0718.

1-(1-Hydroxy-1,3-dihydrobenzo[*c*][1,2]oxaborol-6-yl)guanidine (4). **3**

(13 mg, 0.10 mmol), *N,N*-Di-Boc-1*H*-pyrazole-1-carboxamide (47 mg, 0.15 mmol), DMAP (4 mg, 0.03 mmol) and DIPEA (0.017 mL, 0.10 mmol) were dissolved in MeOH (8 mL). The mixture was allowed to stir for 2 days at room temperature. The solvent was removed *in vacuo* and the resulting residue was dissolved in ethyl acetate. The organic phase was washed with 0.1 N HCl, 1 N NaOH and water. The combined organic phase was dried over anhydrous MgSO₄ and concentrated under reduced pressure. The resulting oil was dissolved in TFA/DCM (1:1, 5 mL) and was stirred for 3 h. The mixture was concentrated and further co-evaporated with several portions of toluene. The residue was purified by preparative HPLC and freeze-dried in water. Obtained as a pale-yellow powder (TFA salt, 5 mg, 16% yield). ¹H NMR (300 MHz, acetone-*d*₆) δ 11.33 (s, 1H), 7.95 (br s, 4H), 7.66 (s, 1H), 7.51 (d, *J* = 8.0 Hz, 1H), 7.44 (d, *J* = 8.1 Hz, 1H), 5.05 (s, 2H). ¹³C NMR (APT, 75 MHz, MeOH-*d*₄/D₂O) δ 147.3, 141.2, 131.3, 122.7, 118.0, 114.8, 69.4. HRMS (ESI): *m/z* [M+H]⁺ calcd for C₈H₁₁BN₃O₂: 192.0940, found: 192.0942.

General Procedure for Amide Coupling in Solution. The respective carboxylic acid (1.0 equiv) and HATU (1.2 equiv) were suspended in DCM (4–25 mL). The mixture was cooled to 0 °C and the respective amine or amine salt (1.0 equiv) was added prior to the dropwise addition of TMP (1.8 equiv). DMF was added until all solids were dissolved and the mixture was stirred at room temperature overnight. All solvents were removed *in vacuo* and the resulting residue was dissolved in ethyl acetate which was washed 2 times with 0.05 N HCl, 0.05 N NaOH and brine. The organic phase was dried over anhydrous MgSO₄, concentrated under reduced pressure and purified by preparative RP-HPLC. After purification, all organic solvents were evaporated and the compounds were freeze-dried in acetonitrile/water.

***N*-(1-Hydroxy-1,3-dihydrobenzo[*c*][1,2]oxaborol-6-yl)hexanamide (5).** 5 was synthesized according to general procedure for amide coupling in solution from hexanoic acid (0.015 mL, 0.12 mmol), HATU (55 mg, 0.15 mmol), 3 (22 mg, 0.12 mmol) and TMP (0.029 mL, 0.22 mmol). Obtained as a colorless powder (20 mg, 68% yield). ¹H NMR (300 MHz, DMSO-*d*₆) δ 9.88 (s, 1H), 9.18 (s, 1H), 8.00 (s, 1H), 7.60 (d, *J* = 8.3 Hz, 1H), 7.31 (d, *J* = 8.2 Hz, 1H), 4.92 (s, 2H), 2.30 (t, *J* = 7.4 Hz, 2H), 1.60 (p, *J* = 7.0 Hz, 2H), 1.38–1.26 (m, 4H), 0.88 (t, *J* = 6.6 Hz, 3H). ¹³C NMR (APT, 75 MHz, DMSO-*d*₆) δ 171.18, 148.40, 138.85, 122.27, 121.39, 120.97, 69.65, 36.32, 30.91, 24.87, 22.56, 13.88. HRMS (ESI): *m/z* [M+H]⁺ calcd for C₁₃H₁₉BNO₃: 248.1455, found: 248.1455.

***N*-(1-Hydroxy-1,3-dihydrobenzo[*c*][1,2]oxaborol-6-yl)-4-(trifluoromethyl)benzamide (6).** 6 was synthesized according to general procedure for amide coupling in solution from 4-(trifluoromethyl)benzoic acid (23 mg, 0.12 mmol), HATU (56 mg, 0.15 mmol), 3 (18 mg, 0.12 mmol) and TMP (0.030 mL, 0.22 mmol). Obtained as a colorless powder (17 mg, 44% yield). ¹H NMR (300 MHz, acetone-*d*₆) δ 9.80 (br s, 1H), 8.25 (s, 1H), 8.22 (d, *J* = 8.2 Hz, 2H), 7.92–7.83 (m, 3H), 7.42 (d, *J* = 8.2 Hz, 1H), 5.02 (s, 2H). HRMS (ESI): *m/z* [M+H]⁺ calcd for C₁₅H₁₁BF₃NNaO₃: 344.0679, found: 344.0680.

4-Amino-*N*-(1-hydroxy-1,3-dihydrobenzo[*c*][1,2]oxaborol-6-yl)benzamide (7). 7 was synthesized according to general procedure for amide coupling in solution from 4-(Boc-amino)benzoic acid (45 mg, 0.19 mmol), HATU (87 mg, 0.23 mmol), 3 (35 mg, 0.19 mmol) and TMP (0.045 mL, 0.34 mmol). The respective Boc protected compound was obtained as a brown oil (37 mg, 53% yield). 20 mg of the oil (0.05 mmol) was stirred in a mixture of TFA/DCM (1:1) for 3 h. All solvents were removed under reduced pressure and the residue was purified by preparative RP-HPLC. After purification, all organic solvents were evaporated and the compounds were freeze-dried in acetonitrile/water. Obtained as a pale-yellow powder (TFA salt, 19 mg, 90% yield). ¹H NMR (300 MHz, ACN-*d*₃) δ 8.72 (s, 1H), 8.08 (s, 1H), 7.80 (d, *J* = 8.7 Hz, 2H), 7.69 (dd, *J* = 8.2, 2.0 Hz, 1H), 7.37 (d, *J* = 8.3 Hz, 1H), 6.90 (d, *J* = 8.7 Hz, 2H), 5.00 (s, 2H). ¹³C NMR (APT, 75 MHz, ACN-*d*₃) δ 166.8, 151.0, 148.3, 138.9, 130.3, 126.4, 125.0, 123.4, 122.6, 116.8, 71.4. HRMS (ESI): *m/z* [M+H]⁺ calcd for C₁₄H₁₄BN₂O₃: 269.1095, found: 269.1100.

***N*-(1-Hydroxy-1,3-dihydrobenzo[*c*][1,2]oxaborol-6-yl)-3-**

methoxybenzamide (9). 9 was synthesized according to general procedure for amide coupling in solution from 3-methoxybenzoic acid (16 mg, 0.11 mmol), HATU (48 mg, 0.13 mmol), 3 (19 mg, 0.11 mmol) and TMP (0.025 mL, 0.19 mmol). Obtained as a colorless powder (12 mg, 41% yield). ¹H NMR (300 MHz, DMSO-*d*₆) δ 10.26 (s, 1H), 9.23 (br s, 1H), 8.16 (s, 1H), 7.77 (dd, *J* = 8.3, 2.0 Hz, 1H), 7.55 (d, *J* = 7.7 Hz, 1H), 7.52–7.41 (m, 2H), 7.39 (d, *J* = 8.2 Hz, 1H), 7.16 (dd, *J* = 8.2, 1.6 Hz, 1H), 4.97 (s, 2H), 3.84 (s, 3H). ¹³C NMR (APT, 75 MHz, DMSO-*d*₆) δ 165.2, 159.2, 149.3, 137.8, 136.4, 129.6, 123.9, 122.5, 121.4, 119.9, 117.2, 112.9, 69.7, 55.3. HRMS (ESI): *m/z* [M+H]⁺ calcd for C₁₅H₁₅BNO₄: 284.1091, found: 284.1085.

***N*-(1-Hydroxy-1,3-dihydrobenzo[*c*][1,2]oxaborol-6-yl)-4-phenoxybenzamide (15).** 15 was synthesized according to general procedure for amide coupling in solution from 4-phenoxybenzoic acid (13 mg, 0.06 mmol), HATU (28 mg, 0.07 mmol), 3 (11 mg, 0.06 mmol) and TMP (0.014 mL, 0.11 mmol). Obtained as a colorless powder (12 mg, 57% yield). ¹H NMR (300 MHz, DMSO-*d*₆) δ 10.23 (s, 1H), 9.22 (s, 1H), 8.16 (s, 1H), 8.01 (d, *J* = 8.8 Hz, 2H), 7.76 (dd, *J* = 8.2, 1.9 Hz, 1H), 7.50–7.41 (m, 2H), 7.38 (d, *J* = 8.3 Hz, 1H), 7.23 (t, *J* = 7.4 Hz, 1H), 7.15–7.07 (m, 4H), 4.97 (s, 2H). ¹³C NMR (APT, 75 MHz, DMSO-*d*₆) δ 164.7, 159.7, 155.6, 149.1, 137.9, 130.3, 129.9, 129.6, 124.4, 123.7, 122.4, 121.4, 119.5, 117.4, 69.7. HRMS (ESI): *m/z* [M+H]⁺ calcd for C₂₀H₁₇BNO₄: 346.1249, found: 346.1235.

***N*-(1-Hydroxy-1,3-dihydrobenzo[*c*][1,2]oxaborol-6-yl)-3-phenoxybenzamide (16).** 16 was synthesized according to general procedure for amide coupling in solution from 3-phenoxybenzoic acid (20 mg, 0.09 mmol), HATU (43 mg, 0.11 mmol), 3 (17 mg, 0.09 mmol) and TMP (0.022 mL, 0.17 mmol). Obtained as a pale-yellow powder (18 mg, 55% yield). ¹H NMR (300 MHz, DMSO-*d*₆) δ 10.31 (s, 1H), 9.22 (br s, 1H), 8.15 (s, 1H), 7.79–7.68 (m, 2H), 7.61 (s, 1H), 7.55–7.36 (m, 4H), 7.29–7.15 (m, 2H), 7.10–7.05 (d, *J* = 8.0 Hz, 2H), 4.96 (s, 2H). ¹³C NMR (APT, 75 MHz, DMSO-*d*₆) δ 164.6, 156.8, 156.3, 149.4, 137.7, 136.8, 132.6, 130.4, 130.2, 124.1, 123.8, 122.8, 122.6, 121.4, 118.9, 117.6, 69.7. HRMS (ESI): *m/z* [M+H]⁺ calcd for C₂₀H₁₇BNO₄: 346.1249, found: 346.1245.

2-(Benzyloxy)-*N*-(1-hydroxy-1,3-dihydrobenzo[*c*][1,2]oxaborol-6-yl)benzamide (17). 17 was synthesized according to general procedure for amide coupling in solution from 35 (19 mg, 0.08 mmol), HATU (39 mg, 0.10 mmol), 3 (15 mg, 0.08 mmol) and TMP (0.020 mL, 0.15 mmol). Obtained as a pale-yellow powder (13 mg, 43% yield). ¹H NMR (300 MHz, DMSO-*d*₆) δ 10.21 (s, 1H), 9.22 (br s, 1H), 8.16 (s, 1H), 7.70 (dd, *J* = 7.6, 1.7 Hz, 1H), 7.58–7.45 (m, 4H), 7.41–7.26 (m, 5H), 7.10 (t, *J* = 7.3 Hz, 1H), 5.26 (s, 2H), 4.94 (s, 2H). ¹³C NMR (APT, 75 MHz, DMSO-*d*₆) δ 164.2, 155.6, 148.9, 137.8, 136.6, 132.0, 129.9, 128.5, 128.1, 127.8, 125.2, 122.4, 121.5, 121.2, 120.8, 113.3, 70.1, 69.7. HRMS (ESI): *m/z* [M+H]⁺ calcd for C₂₁H₁₉BNO₄: 360.1405, found: 360.1404.

3-(Benzyloxy)-*N*-(1-hydroxy-1,3-dihydrobenzo[*c*][1,2]oxaborol-6-yl)benzamide (18). 18 was synthesized according to general procedure for amide coupling in solution from 36 (25 mg, 0.11 mmol), HATU (51 mg, 0.13 mmol), 3 (20 mg, 0.11 mmol) and TMP (0.027 mL, 0.20 mmol). Obtained as a colorless powder (16 mg, 41% yield). ¹H NMR (300 MHz, DMSO-*d*₆) δ 10.25 (s, 1H), 9.22 (br s, 1H), 8.16 (s, 1H), 7.76 (d, *J* = 8.3 Hz, 1H), 7.60 (s, 1H), 7.57 (d, *J* = 7.6 Hz, 1H), 7.51–7.31 (m, 7H), 7.24 (d, *J* = 7.9 Hz, 1H), 5.20 (s, 2H), 4.98 (s, 2H). ¹³C NMR (APT, 75 MHz, DMSO-*d*₆) δ 165.1, 158.2, 149.2, 137.8, 136.8, 136.3, 129.9, 129.5, 128.4, 127.9, 127.7, 123.7, 122.5, 121.4, 120.1, 117.9, 113.9, 69.7, 69.4. HRMS (ESI): *m/z* [M+H]⁺ calcd for C₂₁H₁₉BNO₄: 360.1405, found: 360.1405.

4-(Benzyloxy)-*N*-(1-hydroxy-1,3-dihydrobenzo[*c*][1,2]oxaborol-6-yl)benzamide (19). 19 was synthesized according to general procedure for amide coupling in solution from 4-(benzyloxy)benzoic acid (15 mg, 0.07 mmol), HATU (30 mg, 0.08 mmol), 3 (12 mg, 0.07 mmol) and TMP (0.016 mL, 0.12 mmol). Obtained as a pale-yellow powder (13 mg, 54% yield). ¹H NMR (300 MHz, DMSO-*d*₆) δ 10.14 (s, 1H), 9.22 (br s, 1H), 8.26 (d, *J* = 8.6 Hz, 1H), 8.17 (s, 1H), 7.97 (d, *J* = 8.4 Hz, 2H), 7.82–7.61

(m, 1H), 7.56–7.24 (m, 5H), 7.20–7.02 (m, 2H), 5.21 (s, 2H), 4.96 (s, 2H). ^{13}C NMR (APT, 75 MHz, DMSO- d_6) δ 167.0, 161.9, 149.0, 138.1, 136.7, 136.5, 131.3, 129.6, 128.5, 128.0, 127.8, 123.7, 120.7, 114.6, 69.7, 69.5. HRMS (ESI): m/z $[\text{M}+\text{H}]^+$ calcd for $\text{C}_{21}\text{H}_{19}\text{BNO}_4$: 360.1405, found: 360.1400.

4-((4-Chlorobenzyl)oxy)-N-(1-hydroxy-1,3-dihydrobenzo[*c*][1,2]oxaborol-6-yl)benzamide (20). **20** was synthesized according to general procedure for amide coupling in solution from **38** (22 mg, 0.08 mmol), HATU (38 mg, 0.10 mmol), **3** (16 mg, 0.08 mmol) and TMP (0.020 mL, 0.15 mmol). Obtained as a yellow powder (19 mg, 58% yield). ^1H NMR (300 MHz, DMSO- d_6) δ 10.13 (s, 1H), 9.21 (br s, 1H), 8.15 (s, 1H), 7.96 (d, $J = 8.8$ Hz, 2H), 7.75 (dd, $J = 8.2, 2.0$ Hz, 1H), 7.53–7.45 (m, 4H), 7.37 (d, $J = 7.9$ Hz, 1H), 7.14 (d, $J = 9.0$ Hz, 2H), 5.21 (s, 2H), 4.96 (s, 2H). ^{13}C NMR (APT, 75 MHz, DMSO- d_6) δ 164.8, 159.6, 149.0, 138.0, 135.7, 132.5, 131.3, 129.6, 128.5, 123.6, 122.4, 121.3, 114.5, 69.7, 68.5. HRMS (ESI): m/z $[\text{M}+\text{H}]^+$ calcd for $\text{C}_{21}\text{H}_{18}\text{BClNO}_4$: 394.1016, found: 394.1015.

N-(1-Hydroxy-1,3-dihydrobenzo[*c*][1,2]oxaborol-6-yl)-2-(3-phenoxyphenyl)propanamide (21). **21** was synthesized according to general procedure for amide coupling in solution from 2-(3-phenoxyphenyl)propanoic acid (16 mg, 0.07 mmol), HATU (30 mg, 0.08 mmol), **3** (13 mg, 0.07 mmol) and TMP (0.016 mL, 0.12 mmol). Obtained as a pale yellow powder (12 mg, 48% yield). ^1H NMR (300 MHz, DMSO- d_6) δ 10.08 (s, 1H), 9.18 (br s, 1H), 7.99 (s, 1H), 7.58 (dd, $J = 8.2, 2.0$ Hz, 1H), 7.40–7.30 (m, 4H), 7.22–7.06 (m, 4H), 7.01 (d, $J = 8.0$ Hz, 2H), 4.93 (s, 2H), 3.84 (q, $J = 6.9$ Hz, 1H), 1.41 (d, $J = 6.9$ Hz, 3H). ^{13}C NMR (APT, 75 MHz, DMSO- d_6) δ 171.8, 156.7, 156.5, 148.8, 144.2, 137.9, 130.1, 129.9, 123.5, 122.5, 122.3, 121.5, 121.3, 118.7, 117.5, 116.6, 68.9, 45.7, 18.6. HRMS (ESI): m/z $[\text{M}+\text{H}]^+$ calcd for $\text{C}_{22}\text{H}_{21}\text{BNO}_4$: 374.1562, found: 374.1556.

3-Benzylamino)-N-(1-hydroxy-1,3-dihydrobenzo[*c*][1,2]oxaborol-6-yl)benzamide (22). **22** was synthesized according to general procedure for amide coupling in solution from **46** (21 mg, 0.09 mmol), HATU (42 mg, 0.11 mmol), **3** (17 mg, 0.09 mmol) and TMP (0.022 mL, 0.17 mmol). Obtained as a yellow powder (14 mg, 43% yield). ^1H NMR (300 MHz, DMSO- d_6) δ 10.10 (s, 1H), 8.13 (s, 1H), 7.72 (dd, $J = 8.2, 1.6$ Hz, 1H), 7.42–7.29 (m, 5H), 7.26–7.09 (m, 4H), 6.78 (d, $J = 8.0$ Hz, 1H), 4.96 (s, 2H), 4.34 (s, 2H). ^{13}C NMR (APT, 75 MHz, DMSO- d_6) δ 166.2, 149.5, 148.4, 139.8, 138.0, 135.9, 128.8, 128.3, 127.3, 126.8, 123.7, 122.4, 121.4, 115.4, 115.2, 111.8, 69.7, 46.1. HRMS (ESI): m/z $[\text{M}+\text{H}]^+$ calcd for $\text{C}_{21}\text{H}_{20}\text{BN}_2\text{O}_3$: 359.1565, found: 359.1565.

3-Benzamido-N-(1-hydroxy-1,3-dihydrobenzo[*c*][1,2]oxaborol-6-yl)benzamide (23). **23** was synthesized according to general procedure for amide coupling in solution from **47** (19 mg, 0.08 mmol), HATU (36 mg, 0.10 mmol), **3** (15 mg, 0.08 mmol) and TMP (0.019 mL, 0.14 mmol). Obtained as a beige powder (5 mg, 17% yield). ^1H NMR (300 MHz, DMSO- d_6) δ 10.45 (s, 1H), 10.33 (s, 1H), 9.23 (br s, 1H), 8.18 (s, 1H), 8.05–7.94 (m, 3H), 7.77 (dd, $J = 8.2, 2.0$ Hz, 1H), 7.71 (d, $J = 7.7$ Hz, 1H), 7.62–7.51 (m, 5H), 7.39 (d, $J = 8.2$ Hz, 1H), 4.97 (s, 2H). ^{13}C NMR (APT, 75 MHz, DMSO- d_6) δ 165.7, 165.6, 149.2, 139.3, 137.9, 135.7, 134.7, 131.7, 128.9, 128.6, 128.4, 127.7, 124.4, 123.7, 122.4, 121.4, 120.0, 69.7. HRMS (ESI): m/z $[\text{M}+\text{H}]^+$ calcd for $\text{C}_{21}\text{H}_{18}\text{BN}_2\text{O}_4$: 373.1358, found: 373.1352.

N-(1-Hydroxy-1,3-dihydrobenzo[*c*][1,2]oxaborol-6-yl)-4-morpholinobenzamide (24). **24** was synthesized according to general procedure for amide coupling in solution from 4-morpholinobenzoic acid (22 mg, 0.11 mmol), HATU (49 mg, 0.13 mmol), **3** (22 mg, 0.11 mmol) and TMP (0.025 mL, 0.19 mmol). Obtained as a colorless powder (19 mg, 53% yield). ^1H NMR (300 MHz, DMSO- d_6) δ 10.00 (s, 1H), 9.21 (br s, 1H), 8.12 (s, 1H), 7.89 (d, $J = 8.6$ Hz, 2H), 7.74 (d, $J = 8.7$ Hz, 1H), 7.36 (d, $J = 8.2$ Hz, 1H), 7.02 (d, $J = 8.7$ Hz, 2H), 4.95 (s, 2H), 3.84–3.08 (with solvent signal, m, 8H). ^{13}C NMR (APT, 75 MHz, DMSO- d_6) δ 165.1, 153.3, 148.9, 138.3, 130.9, 129.1, 124.2, 123.8, 122.5, 121.4, 113.5, 69.8, 66.0, 47.4. HRMS (ESI): m/z $[\text{M}+\text{H}]^+$ calcd for $\text{C}_{18}\text{H}_{20}\text{BN}_2\text{O}_2$: 339.1514, found: 339.1509.

3-(4-Fluorophenyl)-N-(1-hydroxy-1,3-dihydrobenzo[*c*][1,2]oxaborol-

6-yl)-5-methylisoxazole-4-carboxamide (25). **25** was synthesized according to general procedure for amide coupling in solution from 3-(4-fluorophenyl)-5-methylisoxazole-4-carboxylic acid (20 mg, 0.09 mmol), HATU (41 mg, 0.11 mmol), **3** (17 mg, 0.09 mmol) and TMP (0.022 mL, 0.16 mmol). Obtained as a yellow powder (12 mg, 37% yield). ^1H NMR (300 MHz, DMSO- d_6) δ 10.47 (s, 1H), 9.25 (br s, 1H), 8.07 (s, 1H), 7.83–7.74 (m, 2H), 7.64 (d, $J = 9.3$ Hz, 1H), 7.43–7.30 (m, 3H), 4.96 (s, 2H), 2.60 (s, 3H). ^{13}C NMR (APT, 75 MHz, DMSO- d_6) δ 170.06, 164.78, 161.50, 159.86, 159.39, 149.65, 137.36, 130.19, 130.07, 124.63, 124.59, 122.90, 121.71, 121.67, 116.10, 115.81, 113.28, 69.72, 11.97. HRMS (ESI): m/z $[\text{M}+\text{H}]^+$ calcd for $\text{C}_{18}\text{H}_{15}\text{BFN}_2\text{O}_4$: 353.1107, found: 353.1091.

(3-(3-(Benzylloxy)benzamido)phenyl)boronic acid (26). **26** was synthesized according to general procedure for amide coupling in solution from **36** (26 mg, 0.11 mmol), HATU (50 mg, 0.13 mmol), (3-aminophenyl)boronic acid (15 mg, 0.11 mmol) and TMP (0.027 mL, 0.20 mmol). Obtained as a colorless powder (22 mg, 58% yield). ^1H NMR (300 MHz, DMSO- d_6) δ 10.15 (s, 1H), 8.03 (s, 2H), 7.84 (d, $J = 8.0$ Hz, 1H), 7.65–7.52 (m, 3H), 7.51–7.28 (m, 8H), 7.23 (dd, $J = 8.0, 2.0$ Hz, 1H), 5.20 (s, 2H). ^{13}C NMR (APT, 75 MHz, DMSO- d_6) δ 164.9, 158.3, 138.2, 136.8, 136.3, 129.6, 129.5, 128.5, 127.9, 127.7, 127.5, 126.7, 122.6, 120.1, 118.0, 113.8, 69.4. HRMS (ESI): m/z $[\text{M}+\text{H}]^+$ calcd for $\text{C}_{20}\text{H}_{19}\text{BNO}_4$: 348.1405, found: 348.1410.

(4-(3-(Benzylloxy)benzamido)methyl)phenyl)boronic acid (27). **27** was synthesized according to general procedure for amide coupling in solution from **36** (18 mg, 0.08 mmol), HATU (38 mg, 0.10 mmol), (4-(aminomethyl)phenyl)boronic acid (12 mg, 0.08 mmol) and TMP (0.019 mL, 0.14 mmol). Obtained as a colorless powder (18 mg, 64% yield). ^1H NMR (300 MHz, DMSO- d_6) δ 9.04 (t, $J = 5.9$ Hz, 1H), 8.02 (s, 1H), 7.74 (d, $J = 7.8$ Hz, 2H), 7.54 (s, 1H), 7.51–7.32 (m, 7H), 7.27 (d, $J = 7.8$ Hz, 2H), 7.17 (dd, $J = 8.0, 2.0$ Hz, 1H), 5.15 (s, 2H), 4.48 (d, $J = 5.8$ Hz, 2H). ^{13}C NMR (APT, 75 MHz, DMSO- d_6) δ 166.1, 158.4, 141.6, 137.0, 135.8, 134.3, 129.7, 128.6, 128.0, 127.8, 126.3, 119.9, 118.0, 113.5, 69.5, 42.8. HRMS (ESI): m/z $[\text{M}+\text{H}]^+$ calcd for $\text{C}_{21}\text{H}_{21}\text{BNO}_4$: 362.1562, found: 362.1555.

6-(Benzylloxy)-N-(1-hydroxy-1,3-dihydrobenzo[*c*][1,2]oxaborol-6-yl)picolinamide (28). **28** was synthesized according to general procedure for amide coupling in solution from **39** (19 mg, 0.08 mmol), HATU (38 mg, 0.10 mmol), **3** (15 mg, 0.08 mmol) and TMP (0.020 mL, 0.15 mmol). Obtained as a brown powder (13 mg, 43% yield). ^1H NMR (300 MHz, DMSO- d_6) δ 10.23 (s, 1H), 9.27 (br s, 1H), 8.21 (s, 1H), 7.96 (t, $J = 7.7$ Hz, 1H), 7.84 (dd, $J = 8.2, 1.8$ Hz, 1H), 7.57–7.21 (m, 6H), 7.15 (d, $J = 8.2$ Hz, 1H), 7.03 (d, $J = 7.7$ Hz, 1H), 5.20 (s, 2H), 4.99 (s, 2H). ^{13}C NMR (APT, 75 MHz, DMSO- d_6) δ 162.0, 161.4, 149.7, 147.4, 140.8, 138.0, 137.3, 134.8, 128.4, 128.1, 126.7, 123.8, 121.6, 115.9, 110.4, 69.8, 46.6. HRMS (ESI): m/z $[\text{M}+\text{H}]^+$ calcd for $\text{C}_{20}\text{H}_{18}\text{BN}_2\text{O}_4$: 361.1358, found: 361.1353.

N-(1-Hydroxy-1,3-dihydrobenzo[*c*][1,2]oxaborol-6-yl)-3-((3-methylbenzyl)oxy)benzamide (29). **29** was synthesized according to general procedure for amide coupling in solution from **40** (17 mg, 0.07 mmol), HATU (32 mg, 0.08 mmol), **3** (13 mg, 0.07 mmol) and TMP (0.017 mL, 0.13 mmol). Obtained as a beige powder (12 mg, 46% yield). ^1H NMR (300 MHz, DMSO- d_6) δ 10.25 (s, 1H), 9.21 (br s, 1H), 8.16 (s, 1H), 7.76 (dd, $J = 8.2, 1.5$ Hz, 1H), 7.63–7.49 (m, 2H), 7.45 (t, $J = 8.0$ Hz, 1H), 7.38 (d, $J = 8.1$ Hz, 1H), 7.32–7.21 (m, 4H), 7.18–7.12 (m, 1H), 5.15 (s, 2H), 4.96 (s, 2H), 2.33 (s, 3H). ^{13}C NMR (APT, 75 MHz, DMSO- d_6) δ 165.1, 158.3, 149.3, 137.8, 137.6, 136.7, 136.4, 129.6, 128.6, 128.4, 128.3, 124.8, 123.8, 122.5, 121.4, 120.1, 117.9, 113.9, 69.7, 69.5, 21.0. HRMS (ESI): m/z $[\text{M}+\text{H}]^+$ calcd for $\text{C}_{22}\text{H}_{21}\text{BNO}_4$: 374.1562, found: 374.1569.

N-(1-Hydroxy-1,3-dihydrobenzo[*c*][1,2]oxaborol-6-yl)-3-((3-methoxybenzyl)oxy)benzamide (30). **30** was synthesized according to general procedure for amide coupling in solution from **41** (22 mg, 0.09 mmol), HATU (39 mg, 0.10 mmol), **3** (16 mg, 0.09 mmol) and TMP (0.020 mL, 0.15 mmol). Obtained as a beige powder (12 mg, 37% yield). ^1H NMR (300 MHz, DMSO- d_6) δ 10.26 (s, 1H), 9.23 (br s, 1H), 8.37 (s, 1H), 7.76

(dd, $J = 8.3, 2.0$ Hz, 1H), 7.62–7.19 (m, 6H), 7.08–6.98 (m, 2H), 6.93–6.84 (m, 2H), 5.17 (s, 2H), 4.97 (s, 2H), 3.77 (s, 3H). ^{13}C NMR (APT, 75 MHz, DMSO- d_6) δ 167.1, 159.4, 158.3, 149.3, 138.4, 137.8, 136.4, 132.2, 129.8, 129.6, 123.8, 122.5, 121.4, 120.2, 119.7, 118.0, 114.9, 114.0, 113.3, 69.7, 69.2, 55.1. HRMS (ESI): m/z [M+H] $^+$ calcd for $\text{C}_{22}\text{H}_{21}\text{BNO}_5$: 390.1511, found: 390.1512.

3-((4-Cyanobenzyl)oxy)-N-(1-hydroxy-1,3-dihydrobenzo[*c*][1,2]oxaborol-6-yl)benzamide (31). **31** was synthesized according to general procedure for amide coupling in solution from **42** (26 mg, 0.10 mmol), HATU (47 mg, 0.12 mmol), **3** (19 mg, 0.10 mmol) and TMP (0.024 mL, 0.18 mmol). Obtained as a pale-yellow powder (10 mg, 26% yield). ^1H NMR (300 MHz, DMSO- d_6) δ 10.26 (s, 1H), 9.22 (br s, 1H), 8.16 (s, 1H), 7.92–7.86 (m, 2H), 7.76 (dd, $J = 8.2, 1.6$ Hz, 1H), 7.63–7.50 (m, 4H), 7.48–7.32 (m, 3H), 7.27 (d, $J = 8.3$ Hz, 1H), 7.25 (d, $J = 8.2$ Hz, 1H), 5.23 (s, 2H), 4.97 (s, 2H). ^{13}C NMR (APT, 75 MHz, DMSO- d_6) δ 167.6, 158.1, 149.3, 140.0, 137.8, 136.4, 133.8, 132.2, 129.8, 127.6, 127.1, 123.8, 122.5, 121.4, 119.7, 117.9, 114.9, 114.0, 69.7, 68.8. HRMS (ESI): m/z [M+H] $^+$ calcd for $\text{C}_{22}\text{H}_{18}\text{BN}_2\text{O}_4$: 385.1358, found: 385.1365.

3-((4-Chlorobenzyl)oxy)-N-(1-hydroxy-1,3-dihydrobenzo[*c*][1,2]oxaborol-6-yl)benzamide (32). **32** was synthesized according to general procedure for amide coupling in solution from **43** (20 mg, 0.08 mmol), HATU (35 mg, 0.09 mmol), **3** (14 mg, 0.08 mmol) and TMP (0.018 mL, 0.14 mmol). Obtained as a pale-yellow powder (18 mg, 60% yield). ^1H NMR (300 MHz, DMSO- d_6) δ 10.25 (s, 1H), 9.22 (br s, 1H), 8.16 (s, 1H), 7.76 (d, $J = 8.2$ Hz, 1H), 7.61–7.41 (m, 7H), 7.39 (d, $J = 8.2$ Hz, 1H), 7.30–7.20 (m, 1H), 5.20 (s, 2H), 4.97 (s, 2H). ^{13}C NMR (APT, 75 MHz, DMSO- d_6) δ 165.1, 158.7, 149.3, 137.8, 136.8, 135.9, 132.5, 129.6, 129.6, 129.5, 128.5, 123.4, 122.5, 121.4, 120.2, 117.9, 114.0, 69.7, 68.6. HRMS (ESI): m/z [M+H] $^+$ calcd for $\text{C}_{21}\text{H}_{18}\text{BClNO}_4$: 394.1016, found: 394.1022.

3-(2,6-Dichlorobenzyl)oxy)-N-(1-hydroxy-1,3-dihydrobenzo[*c*][1,2]oxaborol-6-yl)benzamide (33). **33** was synthesized according to general procedure for amide coupling in solution from **44** (21 mg, 0.07 mmol), HATU (32 mg, 0.09 mmol), **3** (13 mg, 0.07 mmol) and TMP (0.017 mL, 0.13 mmol). Obtained as a pale-yellow powder (19 mg, 63% yield). ^1H NMR (300 MHz, DMSO- d_6) δ 10.26 (s, 1H), 9.21 (br s, 1H), 8.16 (s, 1H), 7.76 (dd, $J = 8.2, 1.4$ Hz, 1H), 7.65 (s, 1H), 7.63–7.54 (m, 3H), 7.50 (d, $J = 7.5$ Hz, 2H), 7.38 (d, $J = 8.6$ Hz, 1H), 7.29 (d, $J = 8.2$ Hz, 1H), 5.33 (s, 2H), 4.97 (s, 2H). ^{13}C NMR (APT, 75 MHz, DMSO- d_6) δ 164.6, 158.3, 149.3, 137.7, 136.5, 136.1, 131.7, 131.5, 129.8, 128.9, 123.8, 122.6, 121.4, 120.6, 117.8, 113.6, 69.8, 65.2. HRMS (ESI): m/z [M+H] $^+$ calcd for $\text{C}_{21}\text{H}_{17}\text{BCl}_2\text{NO}_4$: 428.0626, found: 428.0631.

3-(Cyclohexylmethoxy)-N-(1-hydroxy-1,3-dihydrobenzo[*c*][1,2]oxaborol-6-yl)benzamide (34). **34** was synthesized according to general procedure for amide coupling in solution from **45** (16 mg, 0.07 mmol), HATU (31 mg, 0.08 mmol), **3** (13 mg, 0.07 mmol) and TMP (0.016 mL, 0.12 mmol). Obtained as a beige powder (7 mg, 29% yield). ^1H NMR (300 MHz, DMSO- d_6) δ 10.23 (s, 1H), 9.22 (br s, 1H), 8.15 (s, 1H), 7.76 (dd, $J = 8.1, 2.0$ Hz, 1H), 7.56–7.46 (m, 2H), 7.45–7.34 (m, 2H), 7.21–7.11 (m, 1H), 4.97 (s, 2H), 3.87 (d, $J = 5.9$ Hz, 2H), 1.88–1.60 (m, 6H), 1.36–0.98 (m, 5H). ^{13}C NMR (APT, 75 MHz, DMSO- d_6) δ 166.2, 159.0, 148.2, 138.6, 136.3, 132.9, 129.8, 128.2, 121.4, 121.1, 119.4, 118.1, 113.8, 72.9, 69.7, 37.0, 29.2, 26.1, 25.3. HRMS (ESI): m/z [M+H] $^+$ calcd for $\text{C}_{21}\text{H}_{25}\text{BNO}_4$: 366.1875, found: 366.1869.

4-guanidino-N-(1-hydroxy-1,3-dihydrobenzo[*c*][1,2]oxaborol-6-yl)benzamide (8). **7** (11 mg, 0.03 mmol), *N,N'*-Di-Boc-1*H*-pyrazole-1-carboxamide (13 mg, 0.04 mmol), DMAP (2 mg, 0.01 mmol) and DIPEA (0.005 mL, 0.03 mmol) were dissolved in MeOH (5 mL). The mixture was allowed to stir for 2 days at room temperature. The solvent was removed *in vacuo* and the resulting residue was dissolved in ethyl acetate. The organic phase was washed with 0.1 N HCl, 0.1 N NaOH and water. The organic phase was dried over anhydrous MgSO_4 and concentrated under reduced pressure. The resulting oil was dissolved in TFA/DCM (1:1, 5 mL) and was stirred for 2 h. The mixture was concentrated and further co-evaporated with several portions of toluene. The residue was purified by preparative HPLC and freeze-dried

in water. Obtained as a beige powder (8 mg, 65% yield). ^1H NMR (300 MHz, MeOH- d_4 /D $_2$ O) δ 8.05 (d, $J = 8.1$ Hz, 2H), 7.95 (s, 1H), 7.79 (d, $J = 8.0$ Hz, 1H), 7.47–7.35 (m, 3H), 5.08 (s, 2H). ^{13}C NMR (APT, 75 MHz, MeOH- d_4 /D $_2$ O) δ 164.1, 148.2, 140.5, 138.0, 133.5, 130.8, 125.5, 122.4, 121.0, 115.9, 69.2. HRMS (ESI): m/z [M+H] $^+$ calcd for $\text{C}_{15}\text{H}_{16}\text{BN}_4\text{O}_3$: 311.1313, found: 311.1312.

4-(((1-Hydroxy-1,3-dihydrobenzo[*c*][1,2]oxaborol-6-yl)amino)methyl)benzotrile (10). **3** (15 mg, 0.10 mmol) was dissolved in dry methanol and 4-formylbenzotrile (19 mg, 0.10 mmol) was added. After 1 h, sodium cyanoborohydride (10 mg, 0.15 mmol) was added and the reaction was stirred overnight. The solvents were removed *in vacuo*, the resulting residue was treated with a saturated solution of sodium bicarbonate and extracted 3 times with ethyl acetate. The combined organic phases were dried over anhydrous MgSO_4 , concentrated under reduced pressure and purified by preparative RP-HPLC. After purification, all solvents were evaporated and the compound was freeze-dried in acetonitrile/water. Obtained as a colorless powder (10 mg, 35% yield). ^1H NMR (300 MHz, MeOH- d_4) δ 7.61–7.49 (m, 5H), 7.28 (d, $J = 8.3$ Hz, 1H), 7.24 (d, $J = 8.4$ Hz, 1H), 5.00 (s, 2H), 4.54 (s, 2H). ^{13}C NMR (APT, 75 MHz, MeOH- d_4) δ 141.2, 134.4, 125.1, 124.2, 124.0, 123.8, 120.8, 118.8, 113.9, 109.7, 65.6, 54.7. HRMS (ESI): m/z [M+H] $^+$ calcd for $\text{C}_{15}\text{H}_{14}\text{BN}_2\text{O}_2$: 265.1146, found: 265.1148.

4-Chloro-N-(1-hydroxy-1,3-dihydrobenzo[*c*][1,2]oxaborol-6-yl)benzenesulfonamide (11). A solution of **3** (14 mg, 0.09 mmol) in DCM (5 mL) was cooled on an ice-water bath, *N,N*-diisopropylethylamine (0.048 mL, 0.28 mmol) and 4-chlorobenzenesulfonyl chloride (30 mg, 0.14 mmol) were added. The reaction was warmed to r.t. and stirred overnight. The solvent was removed under reduced pressure. The resulting residue was dissolved in ethyl acetate and washed with water, 0.1 M sodium bicarbonate solution and 1 M HCl. The organic phase was dried over anhydrous MgSO_4 , concentrated under reduced pressure and purified by preparative RP-HPLC. After purification, all organic solvents were evaporated and the compound was freeze-dried in acetonitrile/water. Obtained as a pale-yellow powder (8 mg, 27% yield). ^1H NMR (300 MHz, MeOH- d_4) δ 7.69 (d, $J = 8.7$ Hz, 2H), 7.48 (d, $J = 8.7$ Hz, 2H), 7.32 (s, 1H), 7.26 (d, $J = 7.9$ Hz, 1H), 7.20 (dd, $J = 8.2, 2.0$ Hz, 1H), 5.00 (s, 2H). ^{13}C NMR (APT, 75 MHz, MeOH- d_4) δ 145.8, 143.8, 140.1, 136.6, 133.3, 130.2, 129.9, 126.2, 124.3, 72.0. HRMS (ESI): m/z [M – H] $^-$ calcd for $\text{C}_{13}\text{H}_{10}\text{BClNO}_4\text{S}$: 322.0120, found: 322.0123.

4-Chloro-N-(1-hydroxy-1,3-dihydrobenzo[*c*][1,2]oxaborol-6-yl)-N-methylbenzenesulfonamide (12). A solution of **11** (4 mg, 0.01 mmol) in DMF (1 mL) was cooled on an ice-water bath, K_2CO_3 (4 mg, 0.03 mmol) and iodomethane (3 mg, 0.02 mmol) were added. The reaction was warmed to r.t. and stirred overnight. The solvent was removed under reduced pressure. The resulting residue was dissolved in ethyl acetate and washed with water and 1 M HCl. The organic phase was dried over anhydrous MgSO_4 , concentrated under reduced pressure and purified by preparative RP-HPLC. After purification, all organic solvents were evaporated and the compound was freeze-dried in acetonitrile/water. Obtained as a yellow powder (3 mg, 75% yield). ^1H NMR (300 MHz, MeOH- d_4) δ 7.58–7.47 (m, 4H), 7.18 (d, $J = 8.3$ Hz, 1H), 7.06 (dd, $J = 8.2, 2.3$ Hz, 1H), 6.98 (s, 1H), 5.07 (s, 2H), 3.21 (s, 3H). ^{13}C NMR (APT, 75 MHz, MeOH- d_4) δ 141.6, 139.4, 136.3, 135.2, 130.6, 130.3, 127.5, 124.8, 122.5, 71.4, 36.7. HRMS (ESI): m/z [M+H] $^+$ calcd for $\text{C}_{14}\text{H}_{14}\text{BClNO}_4\text{S}$: 338.0422, found: 338.0413.

1-(1-Hydroxy-1,3-dihydrobenzo[*c*][1,2]oxaborol-6-yl)-3-phenylurea (13). **13** was synthesized in analogy to a previously published method [47]. Phenyl isocyanate (0.010 mL, 0.09 mmol) was added dropwise to a solution of compound **3** (17 mg, 0.09 mmol) in acetone (2 mL). The mixture was stirred overnight and the solvent was removed *in vacuo*. The residue was purified by preparative RP-HPLC. After purification, all organic solvents were evaporated and the compound was freeze-dried in acetonitrile/water. Obtained as a brown powder (11 mg, 44% yield). ^1H NMR (300 MHz, DMSO- d_6) δ 9.10 (br s, 1H), 8.97 (s, 1H), 8.94 (s, 1H), 7.85 (s, 1H), 7.58–7.50 (m, 1H), 7.47 (d, $J = 8.0$ Hz, 2H), 7.30 (d, $J = 7.6$ Hz, 1H), 7.25 (d, $J = 8.0$ Hz, 2H), 6.95 (t, $J = 7.5$ Hz, 1H), 4.93 (s,

2H). ^{13}C NMR (APT, 75 MHz, DMSO- d_6) δ 152.7, 147.3, 140.0, 138.5, 128.7, 125.0, 121.6, 121.5, 119.9, 118.1, 69.6. HRMS (ESI): m/z $[\text{M}+\text{H}]^+$ calcd for $\text{C}_{14}\text{H}_{14}\text{BN}_2\text{O}_3$: 269.1095, found: 269.1093.

Benzyl (1-hydroxy-1,3-dihydrobenzo[*c*][1,2]oxaborol-6-yl)carbamate (14). A solution of **3** (16 mg, 0.09 mmol) in DCM was cooled on an ice-water bath, *N,N*-diisopropylethylamine (0.059 mL, 0.35 mmol), catalytic amounts of 4-dimethylaminopyridine and benzyl chloroformate (0.031 mL, 0.22 mmol) were added. The reaction was warmed to r.t. and stirred overnight. The solvent was removed *in vacuo*. The resulting residue was dissolved in ethyl acetate and washed with water, 1 M sodium bicarbonate solution and 1 M HCl. The organic phase was dried over anhydrous MgSO_4 , concentrated under reduced pressure and purified by preparative RP-HPLC. After purification, all organic solvents were evaporated and the compound was freeze-dried in acetonitrile/water. Obtained as a colorless powder (13 mg, 21% yield). ^1H NMR (300 MHz, DMSO- d_6) δ 9.78 (s, 1H), 9.18 (s, 1H), 7.87 (s, 1H), 7.52 (dd, $J = 8.3$, 2.1 Hz, 1H), 7.47–7.33 (m, 5H), 7.31 (d, $J = 8.3$ Hz, 1H), 5.15 (s, 2H), 4.92 (s, 2H). ^{13}C NMR (APT, 75 MHz, DMSO- d_6) δ 153.5, 148.0, 137.9, 136.7, 128.4, 128.1, 128.0, 127.5, 121.5, 119.9, 69.6, 65.7. HRMS (ESI): m/z $[\text{M}+\text{H}]^+$ calcd for $\text{C}_{15}\text{H}_{15}\text{BNO}_4$: 284.1091, found: 284.1094.

FRET Substrate Synthesis. SARS-CoV-2 M^{pro} , DENV and WNV protease FRET substrate, with the respective sequences 2-Abz-Ser-Ala-Val-Leu-Gln-Ser-Gly-Tyr(3- NO_2)-Arg-OH ($K_m = 536 \mu\text{M}$), 2-Abz-Nle-Lys-Arg-Arg-Ser-Tyr(3- NO_2)-NH $_2$ ($K_m = 106 \mu\text{M}$) and 2-Abz-Gly-Lys-Lys-Arg-Gly-Tyr(3- NO_2)-Ala-Lys-NH $_2$ ($K_m = 36 \mu\text{M}$) were synthesized according to standard Fmoc SPPS procedure, as described before [35]. Purity was determined by RP-HPLC using the same method as for the inhibitors.

SARS-CoV-2 M^{pro} expression and purification. Construct design, expression and purification of SARS-CoV-2 M^{pro} was described before [35]. Overnight culture was grown by shaking at 37 °C in LB medium supplemented with 50 mg/mL kanamycin. On the next day, prewarmed LB medium with kanamycin was mixed 1:40 with overnight culture and bacteria were grown until the optical density (OD) at 600 nm reached 0.3–0.4. Subsequently, the temperature was reduced to 25 °C. Protein expression was induced by addition of 1 mM isopropyl- β -thiogalactoside (IPTG), and cells were further grown by shaking for 24 h at 25 °C. Bacteria were harvested by centrifugation, and the resulting cell pellet was flash frozen in liquid nitrogen and stored for further use at –80 °C. Purification of the SARS-CoV-2 M^{pro} was performed on ice or at 4 °C. One gram of cell pellet was thawed and resuspended in 10 mL of ice-cold buffer A (20 mM Tris, 200 mM NaCl, 10 mM imidazole, pH 7.6). The bacteria were lysed using a high-pressure cell disrupter (One Shot, Constant Systems LTD). Cell debris was centrifuged 2 h at 50,000 g to remove insoluble aggregates and inclusion bodies. The supernatant was mixed after centrifugation with 1 mL of preequilibrated (buffer A) Ni-NTA-beads and incubated on a rolling shaker for 30 min at 4 °C. Subsequently, the Ni-NTA-beads were washed with buffer A, containing increasing concentrations of imidazole (10 mM, 20 mM, 50 mM, pH 7.6; 10–20 mL buffer per step). The protein was eluted by multiple elution steps, each with 1 mL of buffer B (20 mM Tris, 200 mM NaCl, 500 mM imidazole). Elution fractions were analyzed by OD measurement and sodium dodecyl sulfate–polyacrylamide gel electrophoresis. Fractions containing the SARS-CoV-2 M^{pro} were concentrated and buffer was exchanged with buffer C (20 mM Tris, 200 mM NaCl, 1 mM DTT, 1 mM EDTA, pH 7.6) using Amicon centrifugation filters. Protein was further purified by size-exclusion chromatography using an S200 column and buffer C as running buffer. Fractions with pure protein were concentrated and mixed with 50% sterile glycerol, and aliquots were flash frozen in liquid nitrogen and stored at –80 °C until further use.

SARS-CoV-2 M^{pro} Fluorogenic Assay. The SARS-CoV-2 M^{pro} inhibition assays were performed as described before [35]. Continuous enzymatic assays were performed in black 96-well V-bottom plates (Greiner Bio-One, Germany) using a BMG Labtech FLUOstar OPTIMA or a BMG Labtech FLUOstar Omega fluorescence plate reader at an excitation wavelength of 330 nm and an emission wavelength of 430 nm.

Stock solutions of the inhibitors (10 mM in DMSO) were diluted to a final concentration of 50 μM in triplicate and preincubated for 15 min with SARS-CoV-2 M^{pro} (300 nM) in the assay buffer (50 mM Tris-HCl, pH 7.4, 100 mM NaCl, ethylene glycol (20% v/v), 0.0016% Brij 58). The reaction was then initiated by the addition of the FRET substrate (final concentration 25 μM) to obtain a final assay volume of 100 μL per well. The enzymatic activity was monitored for 15 min and determined as a slope of relative fluorescence units per second (RFU/s) for each concentration. Percentage inhibition was calculated relative to a positive control (without the inhibitor), as a mean of triplicates and respective standard deviation. For IC_{50} determinations eight inhibitor concentrations 0–50 μM were chosen for analysis. Dilutions were made starting from 10 mM stock solutions in DMSO, and final concentrations were measured in triplicate. The mean and the standard deviation of the triplicates plotted against the corresponding concentration were used to determine the IC_{50} values on Prism 6.01 (Graphpad Software, Inc.) using nonlinear dose–response curves with variable slopes. All measurements were performed at room temperature.

Dilution Experiment. The fluorimetric assay was performed in black 96-well V-bottom plates (Greiner Bio-One, Germany) using excitation and emission wavelengths of 330 and 430 nm, respectively. The inhibitor in high concentration (100 μM , 100% inhibition) and low concentration (3 μM , $0.5 \times \text{IC}_{50}$) was preincubated with DENV-2 protease (3 μM) in the assay buffer (50 mM Tris-HCl pH 9, ethylene glycol (10% v/v), and 0.0016% Brij 58) for 2 h. The control without inhibitor (equal volume of DMSO) was incubated with the protease accordingly. The preincubated inhibitor and control solutions were pipetted into a 96-well plate together with the assay buffer and additional amount of inhibitor to prepare the final diluted inhibitor solution and the control solutions. The diluted inhibitor solution was prepared by mixing the high-concentration preincubated solution and assay buffer. The protease concentration was 100 nM in the final solutions. The enzymatic reaction was initiated by the addition of the FRET substrate (10 μL , final concentration 50 μM) at 0, 15, 60, and 120 min after the end of the preincubation. The reaction was monitored continuously for 5 min, and the enzymatic activity was determined as slope per second (RFU/s). Percentage inhibition was calculated relative to the control without inhibitor. The measurements were performed in triplicate, and the results are expressed as an average value.

SARS-CoV-2 M^{pro} Mass Adduct Measurement. Selected benzoxaborole compounds and boceprevir at a concentration of 100 μM were incubated with active SARS-CoV-2 M^{pro} (concentration 3 μM) in the assay buffer (50 mM Tris-HCl, pH 7.4, 100 mM NaCl, ethylene glycol (20% v/v), 0.0016% Brij 58). LC-MS measurements were performed on an Agilent 1200 HPLC with an ESI-MS micrOTOF-QII (Bruker Daltonik, Germany) using a Reprosil-Pur ODS-3, Dr. Maisch GmbH, Germany, 3 μm , 50×2 mm HPLC column. The method was as follows: eluent A, water (0.1% formic acid); eluent B, acetonitrile (0.1% formic acid); 0–4.0 min, gradient 10% B to 95% B; 4.1–8.0 min, isocratic 95% B; 8.1–19.0 min, isocratic 10% B; flow rate, 0.3 mL/min. MS measurements were performed in negative mode with external mass calibration and Na-formate as a calibration standard.

Cell Culture. If not stated otherwise, HeLa, Huh-7 and Vero E6 cells were maintained in DMEM supplemented with 100 U/mL penicillin, 100 $\mu\text{g}/\text{mL}$ of streptomycin, and 10% heat-inactivated FCS. During infection of Huh-7 cells, DMEM was supplemented with 10 mM HEPES.

DENV2 Reporter Gene Assay (DENV2proHeLa). The assay was already described in detail [27]. Stable cells were seeded into 96-well plates with a density of 2×10^4 cells per well and treated immediately with inhibitors of dengue virus protease in a final volume of 100 μL . After incubation for 24 h at 37 °C, the medium was removed and cells were lysed by adding 25 μL lysis buffer (Promega) for 15 min at room temperature. Luciferase activity was recorded using a FLUOstar omega plate reader (BMG Labtech) with injections of 100 μL per well coelenterazine (2.75 μM in PBS). Luminescence was recorded for 5 s. Each concentration was assayed in triplicates. Percent inhibition was calculated in

relation to an untreated control. For EC₅₀ calculations data were fitted and calculated with Prism 6.01 (Graphpad Software, Inc.) using a 4-parameter non-linear dose-response curve with background subtraction (wells without cells).

Virus Titer Reduction Assay. Huh-7 cells were seeded into 96-well plates at a density of 1×10^4 cells in 50 μ l per well and incubated overnight. The next day, cells were infected with DENV serotype 2 for 2 h at a MOI of 1, before medium change and compound addition. Infected cells were then incubated for 48 h in the presence of compound in triplicate wells. After 48 h incubation, supernatants were harvested and triplicates pooled. These virus containing supernatants were used to determine the virus titer (reduction) by plaque assay, as described elsewhere [48]. Briefly, VeroE6 cells were seeded into 24-well plates at a density of 2.5×10^5 cells/well and the next day infected for 1 h with 10-fold serial dilutions of virus supernatant ranging from 10^{-1} to 10^{-6} . After medium exchange and addition of the plaque medium, the VeroE6 cells were incubated for 7 days. Cells were subsequently fixed with formaldehyde and plaques visualized by crystal violet stain. At a suitable dilution, plaques were counted, the virus titer calculated and plotted against the respective compound concentration.

Cytotoxicity. Cell viability in Huh-7 or HeLa cells in presence of compound dilutions was determined using CellTiter-Blue® (Promega) according to the manufacturer's instructions. Plates were prepared in parallel to the cell based DENV reporter or virus titer reduction assay with analogous treatment. Each concentration was assayed in triplicates.

Declaration of competing interest

The authors declare that no competing interests exist.

Acknowledgments

We gratefully acknowledge support from Prof. Dr. Ralf Bartenschlager and Marie Bartenschlager for the antiviral activity assays. We thank Heiko Rudy for measuring ESI high resolution spectra, Natascha Stefan and Tobias Timmermann for technical support. This project was supported by the Volkswagen Foundation under grant number 9A836 ("Preclinical development of antiviral protease inhibitors targeting flavin and coronaviruses").

Appendix A. Supplementary data

Supplementary data to this article can be found online at <https://doi.org/10.1016/j.ejmech.2022.114585>.

Abbreviations used

Boc	tert-butoxycarbonyl
DCM	dichloromethane
DENV	dengue virus
DIPEA	<i>N,N</i> -diisopropylethylamine;
DMAP	4-dimethylaminopyridine;
DMEM	Dulbecco's modified eagle medium
DMF	dimethylformamide;
DTT	dithiothreitol
EDTA	ethylenediaminetetraacetic acid
ESI	electrospray ionization
FCS	fetal bovine serum
Fmoc	fluorenylmethyloxycarbonyl
HATU	1-[bis(dimethylamino)methylene]-1 <i>H</i> -1,2,3-triazolo[4,5- <i>b</i>]pyridinium 3-oxide hexafluorophosphate
HCV	hepatitis C virus
HEPES	4-(2-hydroxyethyl)-1-piperazineethanesulfonic acid
HIV	human immunodeficiency virus
IPTG	isopropyl β -d-1-thiogalactopyranoside;

LB	lysogeny broth
MOI	multiplicity of infection
M ^{pro}	3C-like main protease
NS	viral nonstructural protein
PBS	phosphate-buffered saline;
PDE4	phosphodiesterase-4
PLpro	papain-like protease
SARS-CoV-2	severe acute respiratory syndrome coronavirus type 2
TFA	trifluoroacetic acid
TMP	2,4,6-trimethylpyridine,
TOF	Time-of-flight
WNV	West Nile virus
ZIKV	Zika virus

References

- [1] D. Wu, T. Wu, Q. Liu, Z. Yang, The SARS-CoV-2 outbreak: what we know, *Int. J. Infect. Dis.* 94 (2020) 44–48.
- [2] E. Dong, H. Du, L. Gardner, An interactive web-based dashboard to track COVID-19 in real time, *Lancet Infect. Dis.* 20 (5) (2020) 533–534.
- [3] D.R. Owen, C.M.N. Allerton, A.S. Anderson, L. Aschenbrenner, M. Avery, S. Berritt, B. Boras, R.D. Cardin, A. Carlo, K.J. Coffman, A. Dantonio, L. Di, H. Eng, R. Ferré, K.S. Gajiwala, S.A. Gibson, S.E. Greasley, B.L. Hurst, E.P. Kadar, A.S. Kalgutkar, J. C. Lee, J. Lee, W. Liu, S.W. Mason, S. Noell, J.J. Novak, R.S. Obach, K. Ogilvie, N. C. Patel, M. Pettersson, D.K. Rai, M.R. Reese, M.F. Sammons, J.G. Sathish, R.S. P. Singh, C.M. Steppan, A.E. Stewart, J.B. Tuttle, L. Updyke, P.R. Verhoest, L. Wei, Q. Yang, Y. Zhu, An oral SARS-CoV-2 M^{pro} inhibitor clinical candidate for the treatment of COVID-19 374, 2021, pp. 1586–1593, 6575.
- [4] Y. Unoh, S. Uehara, K. Nakahara, H. Nobori, Y. Yamatsu, S. Yamamoto, Y. Maruyama, Y. Taoda, K. Kasamatsu, T. Suto, K. Kouki, A. Nakahashi, S. Kawashima, T. Sanaki, S. Toba, K. Uemura, T. Mizutare, S. Ando, M. Sasaki, Y. Orba, H. Sawa, A. Sato, T. Sato, T. Kato, Y. Tachibana, Discovery of S-217622, a noncovalent oral SARS-CoV-2 3CL protease inhibitor clinical candidate for treating COVID-19, *J. Med. Chem.* 65 (9) (2022) 6499–6512.
- [5] S. Bhatt, P.W. Gething, O.J. Brady, J.P. Messina, A.W. Farlow, C.L. Moyes, J. M. Drake, J.S. Brownstein, A.G. Hoen, O. Sankoh, M.F. Myers, D.B. George, T. Jaenisch, G.R.W. Wint, C.P. Simmons, T.W. Scott, J.J. Farrar, S.I. Hay, The global distribution and burden of dengue, *Nature* 496 (7446) (2013) 504–507.
- [6] M.G. Guzman, S.B. Halstead, H. Artsob, P. Buchy, J. Farrar, D.J. Gubler, E. Hunsperger, A. Kroeger, H.S. Margolis, E. Martinez, M.B. Nathan, J.L. Pelegrino, C. Simmons, S. Yoksan, R.W. Peeling, Dengue: a continuing global threat, *Nat. Rev. Microbiol.* 8 (12) (2010) S7–S16.
- [7] D.J. Gubler, Dengue and dengue hemorrhagic fever, *Clin. Microbiol. Rev.* 11 (3) (1998) 480–496.
- [8] C. Nitsche, S. Holloway, T. Schirmeister, C.D. Klein, Biochemistry and medicinal chemistry of the dengue virus protease, *Chem. Rev.* 114 (22) (2014) 11348–11381.
- [9] S. Ullrich, C. Nitsche, The SARS-CoV-2 main protease as drug target, *Bioorg. Med. Chem. Lett.* 30 (17) (2020), 127377–127377.
- [10] W. Yang, X. Gao, B. Wang, Boronic acid compounds as potential pharmaceutical agents, *Med. Res. Rev.* 23 (3) (2003) 346–368.
- [11] R. Smoum, A. Rubinstein, V.M. Dembitsky, M. Srebnik, Boron containing compounds as protease inhibitors, *Chem. Rev.* 112 (7) (2012) 4156–4220.
- [12] J. Plescia, N. Moitessier, Design and discovery of boronic acid drugs, *Eur. J. Med. Chem.* 195 (2020), 112270.
- [13] U. Bacha, J. Barrila, A. Velazquez-Campoy, S.A. Leavitt, E. Freire, Identification of novel inhibitors of the SARS coronavirus main protease 3CLpro, *Biochemistry* 43 (17) (2004) 4906–4912.
- [14] A. Nocentini, C.T. Supuran, J.-Y. Winum, Benzoxaborole compounds for therapeutic uses: a patent review (2010–2018), *Expert Opin. Ther. Pat.* 28 (6) (2018) 493–504.
- [15] A. Markham, Tavaborole: first global approval, *Drugs* 74 (13) (2014) 1555–1558.
- [16] V. Ramachandran, A. Cline, S.R. Feldman, L.C. Strowd, Evaluating crisaborole as a treatment option for atopic dermatitis, *Expert Opin. Pharmacother.* 20 (9) (2019) 1057–1063.
- [17] R.J. Wall, E. Rico, I. Lukac, F. Zuccotto, S. Elg, I.H. Gilbert, Y. Freund, M.R.K. Alley, M.C. Field, S. Wyllie, D. Horn, Clinical and veterinary trypanocidal benzoxaboroles target, CPSF3 115 (38) (2018) 9616–9621.
- [18] Z. Yin, S.J. Patel, W.-L. Wang, G. Wang, W.-L. Chan, K.R.R. Rao, J. Alam, D. A. Jeyaraj, X. Ngew, V. Patel, D. Beer, S.P. Lim, S.G. Vasudevan, T.H. Keller, Peptide inhibitors of dengue virus NS3 protease. Part 1: Warhead, *Bioorg. Med. Chem. Lett.* 16 (1) (2006) 36–39.
- [19] C. Nitsche, L. Zhang, L.F. Weigel, J. Schilz, D. Graf, R. Bartenschlager, R. Hilgenfeld, C.D. Klein, Peptide-boronic acid inhibitors of flaviviral proteases: medicinal chemistry and structural biology, *J. Med. Chem.* 60 (1) (2017) 511–516.
- [20] J. Lei, G. Hansen, C. Nitsche, C.D. Klein, L. Zhang, R. Hilgenfeld, Crystal structure of Zika virus NS2B-NS3 protease in complex with a boronate inhibitor, *Science* 353 (6298) (2016) 503–505.
- [21] C.Z. Ding, Y.-K. Zhang, X. Li, Y. Liu, S. Zhang, Y. Zhou, J.J. Plattner, S.J. Baker, L. Liu, M. Duan, R.L. Jarvest, J. Ji, W.M. Kazmierski, M.D. Tallant, L.L. Wright, G. K. Smith, R.M. Crosby, A.A. Wang, Z.-J. Ni, W. Zou, J. Wright, Synthesis and

- biological evaluations of P4-benzoxaborole-substituted macrocyclic inhibitors of HCV NS3 protease, *Bioorg. Med. Chem. Lett.* 20 (24) (2010) 7317–7322.
- [22] X. Li, S. Zhang, Y.-K. Zhang, Y. Liu, C.Z. Ding, Y. Zhou, J.J. Plattner, S.J. Baker, W. Bu, L. Liu, W.M. Kazmierski, M. Duan, R.M. Grimes, L.L. Wright, G.K. Smith, R. L. Jarvest, J.-J. Ji, J.P. Cooper, M.D. Tallant, R.M. Crosby, K. Creech, Z.-J. Ni, W. Zou, J. Wright, Synthesis and SAR of acyclic HCV NS3 protease inhibitors with novel P4-benzoxaborole moieties, *Bioorg. Med. Chem. Lett.* 21 (7) (2011) 2048–2054.
- [23] X. Li, Y.-K. Zhang, Y. Liu, C.Z. Ding, Q. Li, Y. Zhou, J.J. Plattner, S.J. Baker, X. Qian, D. Fan, L. Liao, Z.-J. Ni, G.V. White, J.E. Mordaunt, L.X. Lazarides, M. J. Slater, R.L. Jarvest, P. Thommes, M. Ellis, C.M. Edge, J.A. Hubbard, D. Somers, P. Rowland, P. Nassau, B. McDowell, T.J. Skarzynski, W.M. Kazmierski, R. M. Grimes, L.L. Wright, G.K. Smith, W. Zou, J. Wright, L.E. Pennicott, Synthesis and evaluation of novel α -amino cyclic boronates as inhibitors of HCV NS3 protease, *Bioorg. Med. Chem. Lett.* 20 (12) (2010) 3550–3556.
- [24] E.S. Priestley, I. De Lucca, B. Ghavimi, S. Erickson-Viitanen, C.P. Decicco, P1 Phenethyl peptide boronic acid inhibitors of HCV NS3 protease, *Bioorg. Med. Chem. Lett.* 12 (21) (2002) 3199–3202.
- [25] S. Venkatraman, W. Wu, A. Prongay, V. Girijavallabhan, F. George Njoroge, Potent inhibitors of HCV-NS3 protease derived from boronic acids, *Bioorg. Med. Chem. Lett.* 19 (1) (2009) 180–183.
- [26] I.W. Windsor, M.J. Palte, J.C. Lukesh, B. Gold, K.T. Forest, R.T. Raines, Subpicomolar inhibition of HIV-1 protease with a boronic acid, *J. Am. Chem. Soc.* 140 (43) (2018) 14015–14018.
- [27] N. Kühn, D. Graf, J. Bock, M.A.M. Behnam, M.-M. Leuthold, C.D. Klein, A new class of dengue and west nile virus protease inhibitors with submicromolar activity in reporter gene DENV-2 protease and viral replication assays, *J. Med. Chem.* 63 (15) (2020) 8179–8197.
- [28] N. Kühn, M.M. Leuthold, M.A.M. Behnam, C.D. Klein, Beyond basicity: discovery of nonbasic DENV-2 protease inhibitors with potent activity in cell culture, *J. Med. Chem.* 64 (8) (2021) 4567–4587.
- [29] A. Adamczyk-Woźniak, M.K. Cyrański, M. Jakubczyk, P. Klimientowska, A. Koll, J. Kołodziejczak, G. Pojmaj, A. Żubrowska, G.Z. Żukowska, A. Sporzyński, Influence of the substituents on the structure and properties of benzoxaboroles, *J. Phys. Chem.* 114 (6) (2010) 2324–2330.
- [30] A. Adamczyk-Woźniak, I. Madura, A. Pawełko, A. Sporzyński, A. Żubrowska, J. Żyła, Amination-reduction reaction as simple protocol for potential boronic molecular receptors. Insight in supramolecular structure directed by weak interactions, *Cent. Eur. J. Chem.* 9 (2) (2011) 199–205.
- [31] Z. Fu, J. He, A. Tong, Y. Xie, Y. Wei, A convenient and efficient synthesis of dipeptidyl benzoxaboroles and their peptidomimetics, *Synthesis* 45 (20) (2013) 2843–2852.
- [32] M.A.M. Behnam, C.D.P. Klein, Conformational selection in the flaviviral NS2B-NS3 protease, *Biochimie* 174 (2020) 117–125.
- [33] F.G.R. Ehlert, K. Linde, W.E. Diederich, What are we missing? The detergent triton X-100 Added to avoid compound aggregation can affect assay results in an unpredictable manner, *ChemMedChem* 12 (17) (2017) 1419–1423.
- [34] C. Swarbrick, V. Zogali, K.W.K. Chan, D. Kiousis, C.P. Gwee, S. Wang, J. Lescar, D. Luo, M. von Itzstein, M.-T. Matsoukas, G. Panagiotakopoulos, S.G. Vasudevan, G. Rassias, Amidoxime prodrugs convert to potent cell-active multimodal inhibitors of the dengue virus protease, *Eur. J. Med. Chem.* 224 (2021), 113695.
- [35] T. Dražić, N. Kühn, M.M. Leuthold, M.A.M. Behnam, C.D. Klein, Efficiency improvements and discovery of new substrates for a SARS-CoV-2 main protease FRET assay, *SLAS disc. : adv. life sci. R & D* 26 (9) (2021) 1189–1199.
- [36] M.A.M. Behnam, D. Graf, R. Bartenschlager, D.P. Zlotos, C.D. Klein, Discovery of nanomolar dengue and west nile virus protease inhibitors containing a 4-benzoyloxyphenylglycine residue, *J. Med. Chem.* 58 (23) (2015) 9354–9370.
- [37] R. Oerlemans, A.J. Ruiz-Moreno, Y. Cong, N. Dinesh Kumar, M.A. Velasco-Velazquez, C.G. Neochoritis, J. Smith, F. Reggiori, M.R. Groves, A. Dömling, Repurposing the HCV NS3–4A protease drug boceprevir as COVID-19 therapeutics, *RSC Med. Chem.* 12 (3) (2021) 370–379.
- [38] S. Murtuja, D. Shilkar, B. Sarkar, B. Nayan Sinha, V. Jayaprakash, A short survey of Dengue protease inhibitor development in the past 6 years (2015–2020) with an emphasis on similarities between DENV and SARS-CoV-2 proteases, *Biorg. Med. Chem.* (2021), 116415.
- [39] A. Saddique, M.S. Rana, M.M. Alam, A. Ikram, M. Usman, M. Salman, R. Faryal, U. Massab, H. Bokhari, M.S. Mian, A. Israr, Saifullah, Emergence of co-infection of COVID-19 and dengue: a serious public health threat, *J. Infect.* 81 (6) (2020) e16–e18.
- [40] C. Ma, Y. Hu, J.A. Townsend, P.I. Lagarias, M.T. Marty, A. Kolocouris, J. Wang, Ebselen, disulfiram, carmofur, PX-12, tideglusib, and shikonin are nonspecific promiscuous SARS-CoV-2 main protease inhibitors, *ACS Pharmacol. Transl. Sci.* 3 (6) (2020) 1265–1277.
- [41] X. Chen, A. Murawski, K. Patel, C.L. Crespi, P.V. Balimane, A novel design of artificial membrane for improving the PAMPA model, *Pharm. Res. (N. Y.)* 25 (7) (2008) 1511–1520.
- [42] M. Kansy, F. Senner, K. Gubernator, Physicochemical high throughput screening: parallel artificial membrane permeation assay in the description of passive absorption processes, *J. Med. Chem.* 41 (7) (1998) 1007–1010.
- [43] T. Dražić, S. Kopf, J. Corridan, M.M. Leuthold, B. Bertoša, C.D. Klein, Peptide- β -lactam inhibitors of dengue and west nile virus NS2B-NS3 protease display two distinct binding modes, *J. Med. Chem.* 63 (1) (2020) 140–156.
- [44] T. Dražić, N. Kühn, N. Gottscheber, C.N. Hacker, C.D. Klein, The spectrum between substrates and inhibitors: pinpointing the binding mode of dengue protease ligands with modulated basicity and hydrophobicity, *Biorg. Med. Chem.* (2021), 116412.
- [45] M.A. Alam, K. Arora, S. Gurrapu, S.K. Jonnalagadda, G.L. Nelson, P. Kiprof, S. C. Jonnalagadda, V.R. Mereddy, Synthesis and evaluation of functionalized benzoboroxoles as potential anti-tuberculosis agents, *Tetrahedron* 72 (26) (2016) 3795–3801.
- [46] P. Suman, B.P. Patel, A.V. Kasibotla, L.N. Solano, S.C. Jonnalagadda, Synthesis and evaluation of functionalized aminobenzoboroxoles as potential anti-cancer agents, *J. Organomet. Chem.* 798 (2015) 125–131.
- [47] V. Alterio, R. Cadoni, D. Esposito, D. Vullo, A.D. Fiore, S.M. Monti, A. Caporale, M. Ruvo, M. Sechi, P. Dumy, C.T. Supuran, G.D. Simone, J.-Y. Winum, Benzoxaborole as a new chemotype for carbonic anhydrase inhibition, *Chem. Commun.* 52 (80) (2016) 11983–11986.
- [48] P. Metz, A. Chiramel, L. Chatel-Chaix, G. Alvisi, P. Bankhead, R. Mora-Rodriguez, G. Long, A. Hamacher-Brady, N.R. Brady, R. Bartenschlager, Dengue virus inhibition of autophagic flux and dependency of viral replication on proteasomal degradation of the autophagy receptor p62, *J. Virol.* 89 (15) (2015) 8026–8041.